14:02:11 OCA PAD AMENDMENT - PROJECT HEADER INFORMATION 05/15/95

Terminated

Project #: E-25-X44 Cost share #: E-25-349 Rev #: 7
Center # : 10/24-6-R7588-0A0 Center shr #: 10/22-1-F7588-0A0 OCA file #:
Work type : RES
Contract#: MSS-9202932 Mod #: BR DTD 950511 Document : GRANT
Prime #: Contract entity: GTRC

Subprojects ? : Y CFDA:
Main project #: PE #:

Project unit: MECH ENGR Unit code: 02.010.126
Project director(s):
MCDOWELL D L MECH ENGR (404)894-5128
SAXENA A MSE (404)-

Sponsor/division names: NATL SCIENCE FOUNDATION / GENERAL
Sponsor/division codes: 107 / 000

Award period: 920801 to 950131 (performance) 950430 (reports)

Sponsor amount	New this change	Total to date
Contract value	0.00	120,000.00
Funded	0.00	120,000.00
Cost sharing amount		7,500.00

Does subcontracting plan apply ?: N

Title: CRACK GROWTH IN CREEP BRITTLE MATERIALS

PROJECT ADMINISTRATION DATA

OCA contact: Jacquelyn L. Bendall 894-4820

Sponsor technical contact

JEROME SACKMAN
(202)357-9542

NATIONAL SCIENCE FOUNDATION
1800 G STREET, NW
WASHINGTON, DC 20550

Sponsor issuing office

JEFFREY S. LEITHEAD
(202)357-9602

NATIONAL SCIENCE FOUNDATION
1800 G STREET, NW
WASHINGTON, DC 20550

Security class (U,C,S,TS) : U ONR resident rep. is ACO (Y/N): N
Defense priority rating : supplemental sheet
Equipment title vests with: Sponsor GIT

Administrative comments -
ISSUED TO TRANSFER $1,977 TO SUBPROJECT E-18-626.

14:02:12 SUBPROJECTS OF MAIN PROJECT E-25-X44 05/15/95

Project number	Spon/Div	Project Director	Total Contract	Project Unit Total Funded
E-18-626	107/000	SAXENA A	37,539.00	MSE 37,539.00

SR 380

GEORGIA INSTITUTE OF TECHNOLOGY
OFFICE OF CONTRACT ADMINISTRATION

NOTICE OF PROJECT CLOSEOUT

Closeout Notice Date 05/05/95

Project No. E-25-X44 Center No. 10/24-6-R7588-0A0

Project Director MCDOWELL D L School/Lab MECH ENGR

Sponsor NATL SCIENCE FOUNDATION/GENERAL

Contract/Grant No. MSS-9202932 Contract Entity GTRC

Prime Contract No. _____

Title CRACK GROWTH IN CREEP BRITTLE MATERIALS

Effective Completion Date 950131 (Performance) 950430 (Reports)

Closeout Actions Required:	Y/N	Date Submitted
Final Invoice or Copy of Final Invoice	N	
Final Report of Inventions and/or Subcontracts	N	
Government Property Inventory & Related Certificate	N	
Classified Material Certificate	N	
Release and Assignment	N	
Other _____	N	

Comments
LETTER OF CREDIT APPLIES. 98A SATISFIES PATENT REQUIREMENT.

Subproject Under Main Project No. _____

Continues Project No. _____

Distribution Required:

Project Director	Y
Administrative Network Representative	Y
GTRI Accounting/Grants and Contracts	Y
Procurement/Supply Services	Y
Research Property Managment	Y
Research Security Services	N
Reports Coordinator (OCA)	Y
GTRC	Y
Project File	Y
Other _____	N
_____	N

GEORGIA INSTITUTE OF TECHNOLOGY
OFFICE OF CONTRACT ADMINISTRATION

NOTICE OF PROJECT CLOSEOUT (SUBPROJECTS)

Closeout Notice Date 05/05/95

Project No. E-25-X44 Center No. 10/24-6-R7588-0A0_

Project Director MCDOWELL D L_____ School/Lab MECH ENGR_____

Sponsor NATL SCIENCE FOUNDATION/GENERAL_____

Project # E-18-626 PD SAXENA A Unit 02.010.112 T
GRANT # MSS-9202932 MOD# BR DTD 950425 MSE *
Ctr # 10/24-6-R-7588=0A1 Main proj # E-25-X44 OCA CO JLB
Sponsor-NATL SCIENCE FOUNDAT /GENERAL 107/000
CRACK GROWTH IN CREE
Start 920801 End 950131 Funded 35,562.00 Contract 35,562.00

LEGEND
1. * indicates the project is a subproject.
2. I indicates the project is active and being updated.
3. A indicates the project is currently active.
4. T indicates the project has been terminated.
5. R indicates a terminated project that is being modified.

PROGRESS REPORT ON NSF GRANT NO. MSS-9202932
FOR THE PERIOD 8/1/92 - 4/30/93

CRACK GROWTH IN CREEP BRITTLE MATERIALS

Submitted to NSF ENG-MSS Division
Mechanics and Materials Program

DAVID L. MCDOWELL
Professor
George W. Woodruff School of Mechanical Engineering

ASHOK SAXENA
Professor
School of Materials Engineering

Mechanical Properties Research Laboratory
Georgia Institute of Technology
Atlanta, GA 30332

April 30, 1993

BACKGROUND & PROGRAM GOALS/OBJECTIVES

Recent advances in fabrication of components from high temperature materials such as powder metallurgy aluminum alloys, titanium alloys, intermetallics, ceramics and ceramic matrix composites have been very promising. An important limiting factor in the high temperature performance of these materials is time dependent crack growth. Due to limited dislocation mobility within grains, these materials are "creep-brittle," exhibiting grain boundary sliding associated with grain boundary diffusion or viscous glassy phase deformation in the case of ceramics. These materials damage by time-dependent accumulation of cavities or discontinuities on the grain boundaries ahead of the macroscopic crack tip.

This study considers creep crack growth (CCG) of these materials, an area of fracture mechanics which involves materials operating at temperatures in the creep regime (> 0.4 Tm). Widespread agreement does not exist regarding the driving force and time-dependence of creep crack growth during transient, small scale creep conditions in creep ductile materials when the crack tip stress field is rapidly relaxing; this regime, which occurs just after initial loading, load or temperature excursions and, in some cases, crack extension, can be quite significant and is a major focus of this study. Creep crack growth in creep ductile metallic alloys must differ fundamentally from that in creep brittle materials, for example, which exhibit a dominance of viscous grain boundary sliding. The temptation to characterize the crack growth behavior of creep brittle alloys solely in terms of stress intensity factor, for example, belies the complexities of history dependence of crack tip damage, coupled diffusive and dislocation creep mechanisms reflected in load sequence effects, crack growth effects, etc. The bulk of our understanding of creep crack growth behavior is based on response of creep ductile alloys where strain-controlled cavity growth is prevalent.

The goals of this research program are to:

i. understand and quantify the nature of time-dependent stress redistribution and damage evolution ahead of the crack tip for creep brittle materials, including elucidation of appropriate length scales for process zone effects and time scales for crack tip stress redistribution and creep,

ii. establish appropriate local/global crack extension criteria for growing creep cracks in creep brittle materials, including effects of varying load histories,

iii. better understand the nature of transient crack tip effects associated with crack growth and loading changes through a series of experiments and simulations on two different creep-brittle materials, and

iv. determine the influence of process zone crack extension criteria and stress-level dependent rupture criteria, dependent on process zone physics regarding diffusion and/or viscous grain boundary sliding under transient loading conditions and/or crack growth.

We have presently concluded nine months of the two year program, involving a combination of experiments, analysis and numerical simulations of growing cracks to achieve these goals. Appropriately sophisticated constitutive laws for deformation and damage are being implemented to assess length scale and damage effects at the crack tip. Once the time-dependent crack tip fields can be assessed numerically, this information will be used, along with evidence from the experiments, to shed light on appropriate creep crack extension criteria for constant and variable loading histories.

Two creep brittle materials are to be studied in this project. Presently, we are conducting experimental studies of a rapidly solidified, dispersion strengthened Al-Fe-Si-V 8009 alloy. A monolithic ceramic material (e.g. reaction-bonded SiN) is a candidate for the other material.

For creep brittle materials, the following problems must be addressed:

1. The influence of normal stress on facets in addition to the extent of cavitation may be important. Hence, the crack extension criterion may be stress-level dependent. The crack may extend incrementally by "jumping" across several grain boundary facets containing many voids rather than by coalescence of a set of two adjacent voids. The extent of damage within a process zone at the crack tip may be a more appropriate basis for crack extension than critical strain or damage at some fixed distance ahead of the crack tip.
2. The definition of the creep zone used in deriving crack tip stress and strain fields of the HRR type may be modified for the case of creep brittle alloys to provide a more physically-meaningful measure of the expansion rate of the creep zone, valid even for creep exponents below 3.
3. The limits of validity of use of stationary crack solutions for crack tip fields must be established, as must methodologies for growing cracks.
4. Periodic unloading or load changes in actual components may have the effect of altering subsequent creep damage development, reinstating transient near tip fields thereby reducing the domain of validity of K- or C^*-controlled conditions.
5. For linear viscous creep-brittle materials, the distinction between K, C^*, C(t) and C_t is unimportant for stationary cracks. However, for couplings between matrix creep and boundary diffusion, the distinction is relevant and the time-dependence of transient crack tip processes is described differently by these parameters. Furthermore, the use of crack tip parameters at each stage of crack growth which are based on stationary crack solutions is somewhat questionable.
6. The relative extent of diffusion-controlled versus power law creep-controlled cavity growth affects the uniqueness of the correlation.

PROGRESS BY TASK

I. Analytical/computational solutions for stationary and growing cracks:

Work is underway to characterize the creep behavior of the 8009 Al-Fe-Si-V alloy and to determine the constants for an appropriate creep relation over a suitably wide range of stress to represent crack tip field conditions. We have previously developed a two-dimensional finite element code which is routinely used to obtain crack tip, contour integral, and load line displacment rate solutions using either classical elastic-primary-secondary creep with decoupled time-independent plasticity or state variable constitutive laws which couple the two. We are implementing an appropriate nodal release algorithm for crack extension. Most of our studies will be conducted for modest amounts of crack extension, so that a high degree of mesh refinement is not required over the entire remaining ligament. Nevertheless, a very fine mesh will be required ahead of the crack tip along the propagation path. We will impose measured crack velocities which are experimentally observed in Task II and will determine the crack tip field parameters under these conditions to better understand driving forces for creep crack growth under constant K and variable K loading conditions. Mr. Kangmin Niu, a Ph.D. student in Mechanical Engineering is responsbile for carrying out the work in this task.

In limited calculations, cavity growth will be considered to assess the growth of damage in addition to the character of the creep zone. It is important to note that in full field solutions, damage will be assumed to be localized in the near tip region and small strain analysis will be undertaken. The validity of these assumptions will be assessed.

These aforementioned analyses will serve to provide a basis for formulation of a global and/or local approach for creep crack growth for creep brittle materials. To better understand the behavior of creep cracks at low stress levels dominated by diffusion, the singular elastic stress field will be used to generate far field boundary conditions for the case of linear viscous response. Both static and varying loading will be considered. We are aiming to develop a discrete (granular flow) model with diffusional/viscous flow grain boundary representation and finite strain provisions to determine the crack tip domain of extreme stress redistribution (stress shielding).

II. Experiments on two model creep brittle materials:

The experimental program is being conducted in the Mechanical Properties Research Laboratory at Georgia Tech. The test matrix consists of isothermal smooth specimen creep tests at several stress levels, constant load creep crack growth experiments on C(T) type specimens and sequential step loading of C(T) type specimens. Quantitative metallography and ceramography will be employed to assess damage in failed specimens. The crack extension history, loading, crack opening displacements and load line deflection rates will be recorded.

A M.S. student in Materials Science and Engineering, Ms. Kimberly Jones, has been investigating the creep deformation and crack growth behavior of a dispersion strengthened Al-Fe-Si-V alloy 8009 at test temperatures of 316 °C and 150 °C. Some preliminary results

from tests completed at 316 °C are described here.

The creep deformation behavior for stress levels ranging from 85.4 to 107.0 MPa are shown in Figure 1. Figure 1a shows the entire creep strain versus time data while Figure 1b highlights the first 150 hours of the tests during which primary creep behavior is dominant. The observations made from these data are as follows:

i. Primary creep strains contribute significantly to the deformation behavior at all stress levels investigated. Therefore, any models for representing the creep deformation behavior must include the influence of primary creep.

ii. A sudden change in the creep deformation kinetics occurs when the stress is increased from 100.6 MPa to 107.0 MPa.

The following equation may be used to represent the creep data as a function of time:

$$\varepsilon = [(1+p)A_1 t]^{1/(1+p)}(\sigma/\sigma_o)^{n_1} + A_2(\sigma/\sigma_o)^{n_2}t + A_3(\sigma/\sigma_o)^{n_3}t$$

Here, ε is the strain, σ is the stress, and t is time. The various constants were developed from regression analysis of the data:

σ_o = 179.2 MPa (yield strength of the material at 316° C)
p = 2
$A_1 = 6 \times 10^{-4}$
$n_1 = 6.6$
$A_2 = 8 \times 10^{-8}$
$n_2 = 2.1$
$A_3 = 2 \times 10^{9}$
$n_3 = 54.9$

The above constants have been determined assuming time t in hours. The fitted lines are shown with the actual data at the various stress levels. The constants appear to represent the data well. It is also noted that the slope of the secondary creep rate for stress levels less than 100.6 MPa is 2.1 indicating that creep mechanisms are diffusion-controlled. However, the creep exponent rises sharply for stress levels between 100.6 and 107 MPa. This could be due to decohesion between the dispersoids and the matrix after the accumulation of the primary creep strain. This would cause the local effective stress in the matrix to rise sharply and may trigger tertiary creep behavior, resulting in the accelerated creep rates. This will be investigated further using scanning and transmission microscopy.

The creep crack growth rates from compact specimens loaded to different initial stress intensity levels are shown in Figures 2 and 3. In Figure 2, the creep crack growth rates are correlated with C_t and in Figure 3 the same data are correlated with K. The da/dt correlates well with K if the first data points are excluded from the results of the two

specimens tested at the lowest initial K levels. It can be postulated that during the initial portions of these tests, the crack growth rate is slow in comparison with the expansion rate of the creep zone due to the high primary creep rates. Thus, the crack growth rates in this region may be better described by C_t instead of K.

The above results will be modelled using finite element analyses as described previously. The results of these analyses will be used to develop an understanding of the crack growth behavior and to recommend the most appropriate crack tip parameter for correlating creep crack growth rates. The crack surfaces and the damage in the crack tip region will be investigated to understand the micromechanisms of creep crack growth in these materials. Potential instabilities in the microstructure will also be investigated using TEM.

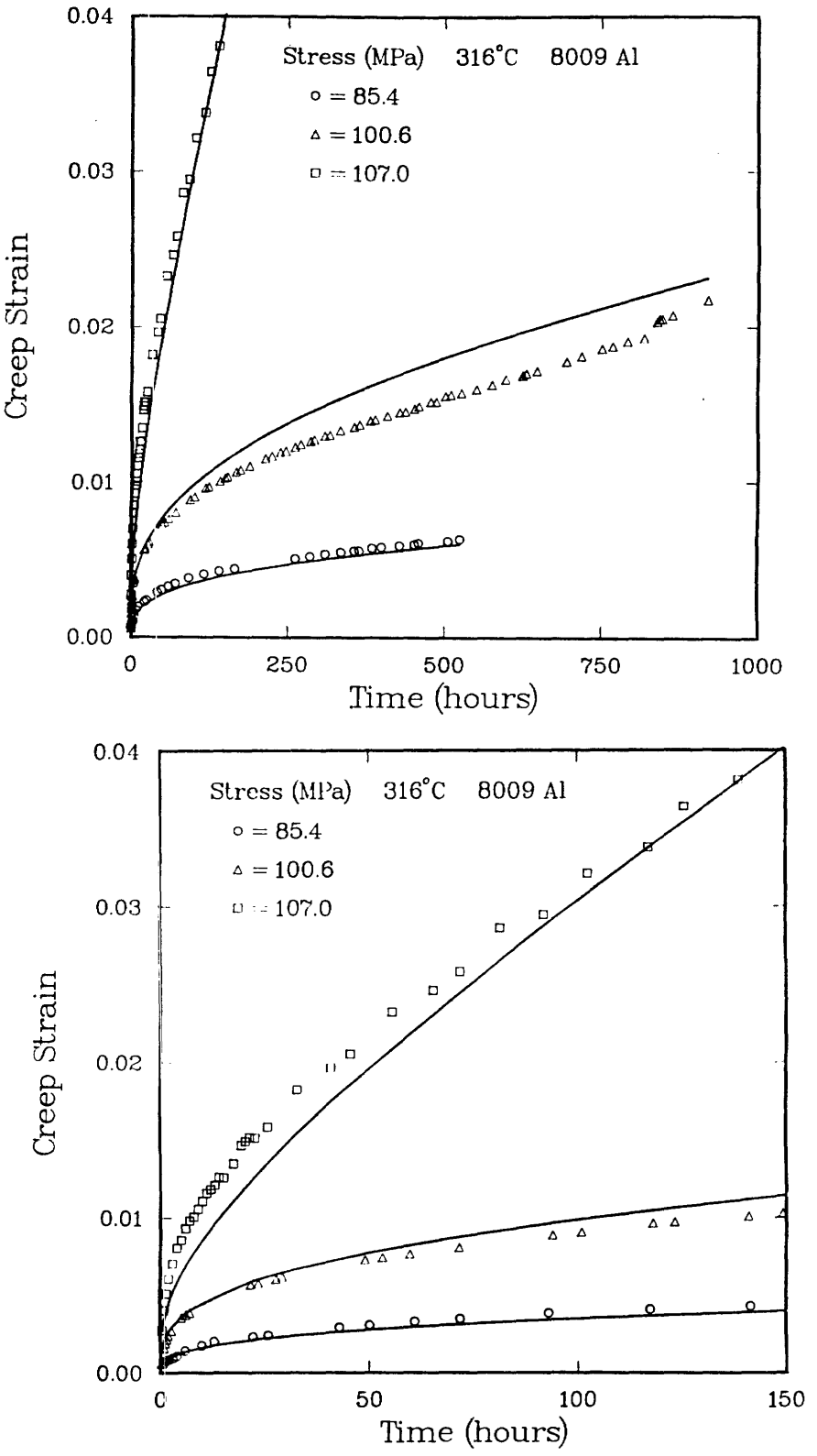

Fig. 1 Creep deformation behavior of Al alloy 8009 at 316° C: (a) data collected on three specimens, and (b) the initial portion of the data. The solid lines are results of the regression fits of the model for representing creep behavior.

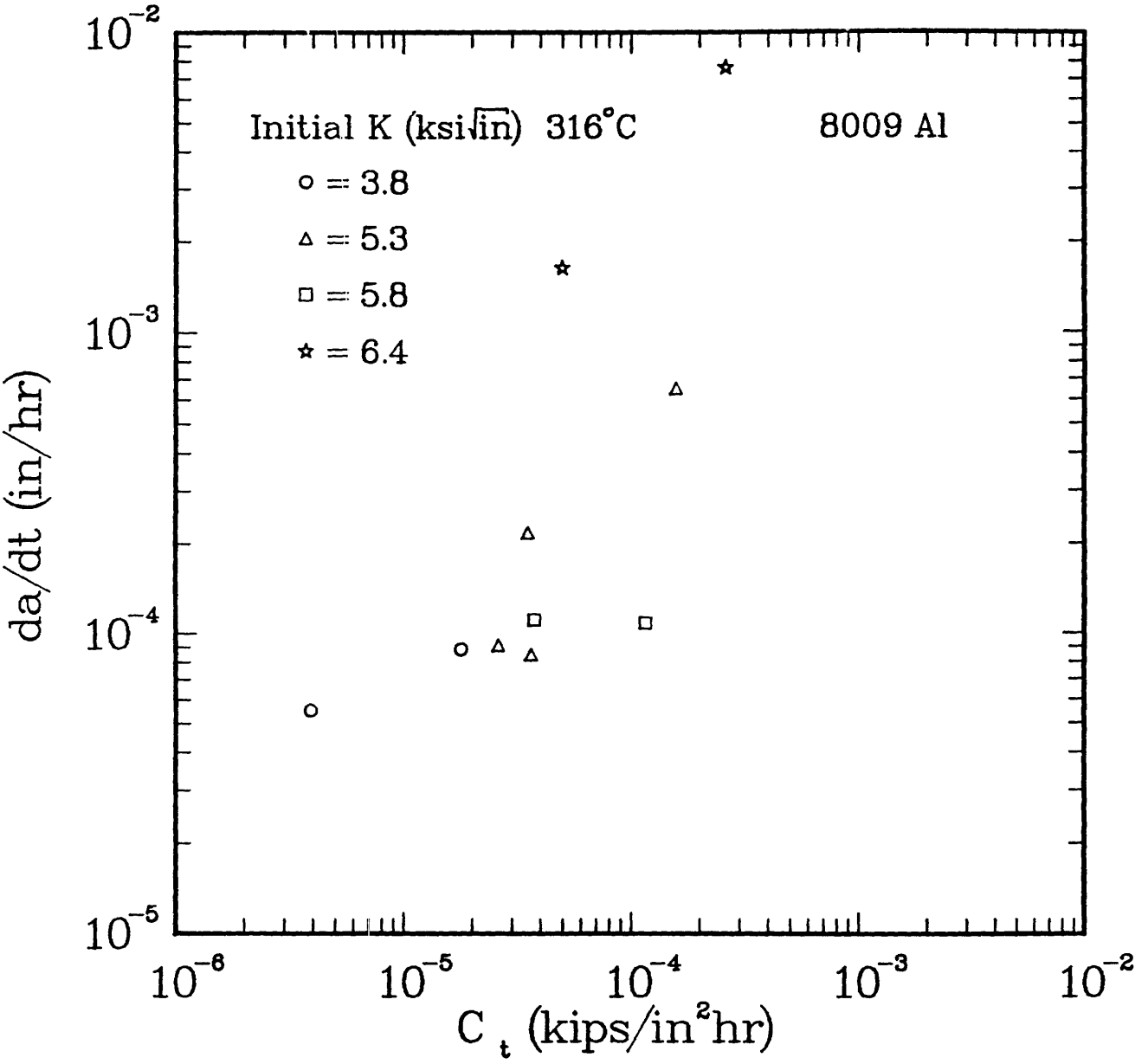

Fig. 2 Creep crack growth rate as function of the C_t parameter for four compact type specimens tested at different initial K levels.

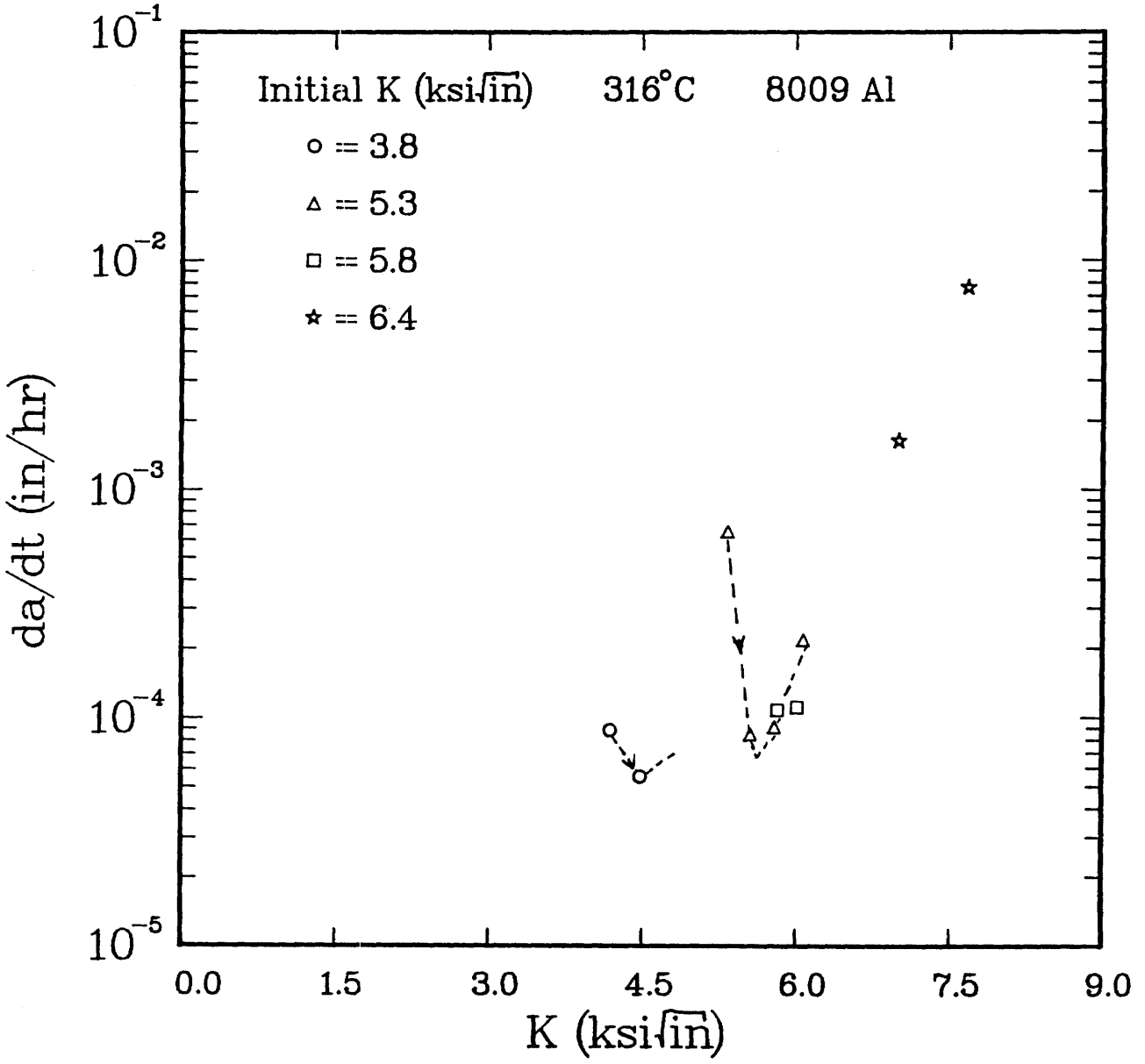

Fig. 3 Creep crack growth rate as a function of the stress intensity parameter, K, for four compact type specimens tested at different initial K levels.

OMB Number 345-0058

NATIONAL SCIENCE FOUNDATION
4201 Wilson Blvd.,
Arlington, VA 22230

BULK RATE
POSTAGE & FEES PAID
National Science Foundation
Permit No. G-69

PI/PD Name and Address

David L. McDowell
Department of Mechanical Engineering
GA Tech Res Corp - GIT
School of Mechanical Engineering
Atlanta GA 30332-0405

NATIONAL SCIENCE FOUNDATION
FINAL PROJECT REPORT

PART I - PROJECT IDENTIFICATION INFORMATION

1. Program Official/Org.	Oscar Dillon - CMS
2. Program Name	MECHANICS & MATERIALS PROGRAM
3. Award Dates (MM/YY)	From: 08/92 To: 01/95
4. Institution and Address	GA Tech Res Corp - GIT Administration Building Atlanta GA 30332
5. Award Number	9202932
6. Project Title	Crack Growth in Creep Brittle Materials

This Packet Contains
NSF Form 98A
And 1 Return Envelope

PART IV -- FINAL PROJECT REPORT -- SUMMARY DATA ON PROJECT PERSONNEL

(To be submitted to cognizant Program Officer upon completion of project)

The data requested below are important for the development of a statistical profile on the personnel supported by Federal grants. The information on this part is solicited in resonse to Public Law 99-383 and 42 USC 1885C. All information provided will be treated as confidential and will be safeguarded in accordance with the provisions of the Privacy Act of 1974. You should submit a single copy of this part with each final project report. However, submission of the requested information is not mandatory and is not a precondition of future award(s). Check the "Decline to Provide Information" box below if you do not wish to provide the nformation.

Please enter the numbers of individuals supported under this grant.
Do not enter information for individuals working less than 40 hours in any calendar year.

	Senior Staff		Post-Doctorals		Graduate Students		Under-Graduates		Other Participants[1]	
	Male	Fem.	Male	Fem.	Male	Fem.	Male	Fem.	Male	Fem.
A. Total, U.S. Citizens	2				1	1				
B. Total, Permanent Residents										
U.S. Citizens or Permanent Residents[2]:										
American Indian or Alaskan Native										
Asian.....										
Black, Not of Hispanic Origin.....										
Hispanic										
Pacific Islander										
White, Not of Hispanic Origin										
C. Total, Other Non-U.S. Citizens										
Specify Country 1. China						1				
2.										
3.										
D. Total, All participants (A + B + C)	2				1	2				
Disabled[3]										

☐ Decline to Provide Information: Check box if you do not wish to provide this information (you are still required to return this page along with Parts I-III).

[1] Category includes, for example, college and precollege teachers, conference and workshop participants.

[2] Use the category that best describes the ethnic/racial status fo all U.S. Citizens and Non-citizens with Permanent Residency. *(If more than one category applies, use the one category that most closely reflects the person's recognition in the community.)*

[3] A person having a physical or mental impairment that substantially limits one or more major life activities; who has a record of such impairment; or who is regarded as having such impairment. *(Disabled individuals also should be counted under the appropriate ethnic/racial group unless they are classified as "Other Non-U.S. Citizens.")*

AMERICAN INDIAN OR ALASKAN NATIVE: A person having origins in any of the original peoples of North America and who maintains cultural identification through tribal affiliation or community recognition.

ASIAN: A person having origins in any of the original peoples of East Asia, Southeast Asia or the Indian subcontinent. This area includes, for example, China, India, Indonesia, Japan, Korea and Vietnam.

BLACK, NOT OF HISPANIC ORIGIN: A person having origins in any of the black racial groups of Africa.

HISPANIC: A person of Mexican, Puerto Rican, Cuban, Central or South American or other Spanish culture or origin, regardless of race.

PACIFIC ISLANDER: A person having origins in any of the original peoples of Hawaii; the U.S. Pacific territories of Guam, American Samoa, and the Northern Marinas; the U.S. Trust Territory of Palau; the islands of Micronesia and Melanesia; or the Philippines.

WHITE, NOT OF HISPANIC ORIGIN: A person having origins in any of the original peoples of Europe, North Africa, or the Middle East.

FINAL REPORT
NSF AWARD NO. 9202932

CRACK GROWTH IN CREEP-BRITTLE MATERIALS

Submitted to Mechanics and Materials Program
Oscar Dillon - CMS
National Science Foundation

Submitted by

DAVID L. MCDOWELL
Professor
George W. Woodruff School of Mechanical Engineering

ASHOK SAXENA
Professor
School of Materials Science and Engineering

May 1995

INTRODUCTION

At elevated temperatures, components can exhibit significant time-dependent inelastic deformation. Creep crack growth (CCG) is an area of fracture mechanics which involves materials operating at temperatures in the creep regime (> 0.4 Tm). This subject has evolved in recent years through analogy with elastic-plastic fracture mechanics approaches for crack tip stress and strain fields, as well as development of global parameters which can be experimentally measured to characterize the strength of these fields.

Recent thrusts in high temperature materials involve fabrication of components from powder metallurgy aluminum alloys, titanium alloys, intermetallics, ceramics and ceramic matrix composites. An important limiting factor in the high temperature performance of these materials is time dependent crack growth. Due to limited dislocation mobility within grains, these materials are "creep-brittle." The dependence of damage nucleation on stress appears to be a defining characteristic of these materials, in contrast to creep-ductile alloys in which cavities nucleate and grow via predominantly strain driven mechanisms.

High temperature creep crack growth under sustained loading may be classified as either creep-ductile or creep-brittle, depending on the extent of creep deformation which accompanies crack growth. Creep-ductile materials are characterized by crack growth rates that are slow compared to the rate of expansion of creep zone, resulting in extensive accumulation of creep deformation in the cracked body. In contrast, creep-brittle materials are characterized by crack growth rates comparable to the rate of expansion of the creep zone, resulting in development of a narrow, ribbon-like wake of creep deformation along the crack path. Crack growth effects have been largely neglected in creep crack growth mechanics, due primarily to the predominant consideration of creep-ductile materials in previous studies; for these materials, the assumption of stationary crack solutions for the crack tip fields at each stage of crack growth is reasonably accurate. Creep-brittle alloys, however, defy this simplicity and crack growth effects therefore greatly complicate the issue of correlation of creep crack growth. Creep-brittle materials typically exhibit a significant incubation period, followed by a fairly rapid crack growth rate up to failure. The creep strain to failure is on the order of a few percent. As such, their behavior is to some degree analogous to that of fracture of brittle materials that exhibit little inelastic behavior prior to abrupt failure.

Two classes of creep-brittle materials can be identified. One class involves very low creep exponents ($n < 3$), such that K-controlled steady state growth conditions may be favored. Many structural ceramics and intermetallics may fall into this category. Another class of creep-brittle materials are powder metallurgy alloys and other high strength alloys which involve stress level dependence of damage nucleation; in this case, the creep law often exhibits distinct regimes with radically different slopes, indicative of a threshold crack tip stress over some length scale necessary to nucleate cavitation, promoting subsequent rapid creep. Below this threshold stress level, the steady state creep exponent is on the order of 5-8; above it, it climbs to 20-30.

Time-dependent fracture research has leaned heavily toward understanding the fracture behavior of creep-ductile materials. Recently, however, the creep crack growth

characteristics of several creep-brittle materials have been investigated to address the potential use of these materials in critical applications (primarily aerospace) (cf. [1-4]). These investigations have generally concluded that the stress intensity factor, K, is more appropriate than time-dependent fracture parameters for correlating creep crack growth rate in creep-brittle materials. While it appears that the issues surrounding the choice of the optimum correlating parameters for characterizing creep crack growth in creep-ductile materials is reaching a degree of consensus, much more understanding of the creep crack growth behavior in creep-brittle materials is required.

This research has sought to gain insight into the driving force-material resistance balance for these materials, and to understand the potential for correlation of creep crack growth rate with far-field fracture parameters. A combined experimental-computational study has been undertaken to reach the following goals:

1. understand and quantify the nature of damage and stress redistribution ahead of the crack tip for creep-brittle materials, and

2. establish appropriate local/global crack extension criteria for growing creep cracks in creep-brittle materials.

For creep-brittle materials, the following issues must be addressed:

1. The crack extension criterion is not governed purely by cumulative creep strain, but involves an additional stress level dependence.
2. There is a considerable period of damage incubation for a virgin cracked body subjected to load at high temperature, after which crack growth is rapid. The incubation period may in some cases comprise the majority of life.
3. Since the crack growth rate is on the order of the rate of creep zone expansion at the crack tip, the crack tip fields are not self-similar as the crack extends; moreover, a relative strong history dependence results.
4. Some creep-brittle materials exhibit a transition from creep-ductile to creep-brittle growth conditions, even for a given level of applied loading.

In the following sections, we outline both experimental and computational accomplishments of this research program which relate to these issues. These two components of the program have been vitally linked via close collaboration of the PIs and their graduate students.

EXPERIMENTAL STUDIES

The experiments were conducted in the Mechanical Properties Research Laboratory (MPRL) at Georgia Tech. Three model materials were utilized as test materials in this program. They were (1) rapidly solidified Al alloy 8009 (2) reaction bonded silicon nitride reinforced with Nicalon fibers and (3) C-Mn steel which shows rapid creep crack growth behavior at temperatures in the range of 360°C. The experimental results on the C-Mn materials were available as part of a program supported by Babcock and Wilcox at Georgia Tech. Under NSF support, numerical analyses of some of the tests were performed to understand the creep crack growth behavior. A brief description of the three materials is provided followed by some salient experimental results.

Rapidly Solidified Al Alloy 8009: Rapidly solidified dispersion strengthened aluminum alloys (RSAA) are thermally stable at temperatures in excess of 300°C and are therefore candidate materials for light weight high temperature structures. The chemical composition consists of 8.5% Fe, 2.3%V. 1.7%Si and balance Al. The test material was donated by the NASA Langley Research Center. Rapid solidification is achieved by cooling at rates up to 10^5 K/sec by a method called planar flow casting which produces 25 μm thick strips of material. These strips are subsequently pulverized into powder and then consolidated into billets which are either forged or extruded to achieve full densification. The material consists of 30 - 80 nm diameter dispersoids with a volume fraction of 25 percent. The creep ductility of this material is on the order of several percent.

SiC fiber/Si_3N_4 Composite:

The continuous silicon carbide fiber reinforced silicon nitride matrix composite plates used in the present work were manufactured using the reaction sintering technique. In this technique, developed by Dr. T. L. Starr of Georgia Tech, the attritor-milled silicon metal powder with an average diameter of 0.2 to 0.5 μm was combined with the ceramic grade Si-C-O Nicalon fiber. Then the formed green composite was sintered at a high temperature up to 1200°C in the N_2 atmosphere to convert Si into its nitride. The fiber volume fraction was 15% and the predominant phase in the reaction sintered matrix is α - Si_3N_4. The as-received Nicalon fiber is a homogeneous mixture of amorphous Si-C-O compounds. During the high temperature sintering process, certain amounts of C and O evaporates and crystallization occurs. Thus, the remaining component of the fiber in the composite is the SiC crystal with fine grain size.

C-Mn Steel: The test materials consisted of carbon steel used in manufacturing intermediate temperature piping. The material was taken from a manufactured pipe which was strained 15 percent at room temperature and subsequently aged for 8 hours at 343°C. This condition was known as the aged condition. The microstructure consisted of equiaxed pearlite colonies in a ferrite matrix. A part of this material was also subjected to a normalizing heat treatment, consisting of exposure to a temperature of 900°C for 1.5 hours. This condition is referred to as normalized condition, with a microstructure very similar in appearance to that of the aged condition.

Creep Deformation and Crack Growth Behavior

Al Alloy 8009:

Figure 1 shows the creep strain as a function of time at the test temperature of 316°C for aluminum alloy 8009. Figure 2 shows the steady-state creep rate as a function of stress. The usual power-law which describes the behavior of conventional metals does not apply to this material. There appears to be a distinct change in slope which occurs at a stress of approximately 100MPa. The creep ductility decreased with increasing failure time, Fig. 3.

Figure 4 shows the creep crack growth rate as a function K. In all tests, the da/dt first decreases with K and then it increases. The decrease in da/dt with K during the initial portion of the tests is attributed to rapid stress redistribution due to expansion of the creep zone. Therefore, in this portion of the test, no correlation between da/dt and K is expected. This point will be explained further with the aid of the numerical results. Figure 5 shows the same data plotted as a function of C_t, a stress power release rate type parameter. However, this correlation does not hold for portions of the test during which the crack growth rate increases. The data from the increasing crack growth portion of the various tests is plotted in Fig. 6 and it does appear to correlate better with K. Also shown in Fig. 6 are results from tests performed at 150°C. At this temperature, the alloy exhibits a ductility minimum. We also observe that the crack growth rates at 150°C for comparable initial K values are more rapid than the rates measured at 316°C. The creep crack growth rates, as expected, increase or decrease with creep ductility. These very interesting results are discussed in a forthcoming paper.

The creep crack growth in alloy 8009 occurs by nucleation and growth of cavities. This was established by extensive metallographic and fractographic studies. Figure 7 shows the distribution of cavity diameter as a function of creep crack extension. The fractographs clearly showed that cavities grew around dispersoids. However, each dispersoid did not cause a cavity to nucleate around it. This was confirmed by the observation that cavity diameters ranged from 3 to 10 μm (Fig. 7) while the average dispersoid spacing was only 0.1 μm. The cavities appeared to have coalesced with each other, indicating the local fracture mode to be very ductile. This fracture mode was also consistent with that obtained in creep rupture specimens. A definite correlation was also observed between the cavity diameter and the crack tip parameter. This interesting result will be discussed in detail in a forthcoming paper.

SiC Fiber/Si_3N_4 Composite:

To date, a few creep crack growth tests have been completed on this material. The data analysis has not been conducted to report the results. The high temperature tests were conducted at 1000°C. Solid-state phase transformation as well as oxidation at the fiber-matrix interface were detected in this material at 1000°C. Dimensional changes accompanying the solid-state transformations made it difficult to interpret the load-line deflection data for purposes of calculation of field parameters. However, definite changes in the crack growth morphology were observed at elevated temperature. Compared to room temperature, the crack growth at elevated temperature was accompanied by significantly less

delamination. This made the crack growth process appear to be quite self-similar. Thus, the crack growth is much more likely to be correlated with a crack tip parameter under such conditions. In this ongoing research, we are currently attempting to find a temperature at which the reaction bonded silicon nitride is more thermally stable and then utilize that temperature for creep crack growth testing. The results of this research will be summarized in a paper to be completed in June of 1995. The objective of the study is to characterize the mechanisms of creep crack extension and subsequently evaluate the most promising approaches for correlating crack growth in these materials.

C-Mn Steel:

The test results described in this section were obtained under a separate study sponsored at Georgia Tech by Babcock and Wilcox. Since the behavior of these materials was creep-brittle in nature, finite element simulation of some of these tests was carried out under this program. Therefore, some important experimental results are described in this section.

Figure 8 shows the creep strain as a function of time at various stress levels for the aged material and Fig. 9 shows the secondary creep rate as a function of stress. The strain rate versus stress behavior is similar to that observed for the Al alloys with two characteristic slopes. Figures 10 and 11 show the creep crack growth rates correlated with K and C_t, respectively. The correlation is clearly much better with K for both the normalized and the aged conditions, which is typical of creep-brittle conditions. These results were investigated using finite element simulations of growing cracks as described later in this report.

COMPUTATIONAL STUDIES

Finite element analyses were carried out using a small strain code developed by Leung and McDowell [5] based on an implicit trapezoidal time stepping scheme. The code includes accuate integration of viscoplastic constitutive equations which may include, for example, elasticity, plasticity, primary and secondary creep. Most importantly, crack growth effects are realistically treated with the code. In this work, experimentally determined creep crack growth rates were imposed in the simulations to gain an understanding of the crack tip stresses and strains, crack tip field parameters, and the history dependence of these fields.

Crack growth is simulated by releasing a sequence of finite element nodes along the crack growth path at a specified rate using an algorithm similar to those of Hawk and Bassani [6] and Moyer and Liebowitz [7]. As the crack grows from one nodal position to the next, the net force on the node to be released is gradually relaxed over a number of time steps. Instead of releasing the node over a prescribed number of force decrements, an opening displacement is imposed on the node to be released to ensure that the rate of force release due to crack growth is faster than the rate of force relaxation due to creep. Application of these displacement increments ensures that the crack immediately begins to open. Increments of displacement are continued (based on the previously released nodes overall y-direction displacement) until the net force on the node is reduced to a fraction of its original value or until a specified time is reached. The remaining force on the node is

then reduced to zero by applying force decrements over a number of time steps.

The new variable time step, nodal release approach devised here selects a new time step for each displacement increment or load decrement according to the most conservative of three time stepping criteria. First, the effective creep strain expected to be accumulated at any gauss point during the current time step should be less than or equal to some fraction (τ) of the total effective strain at that gauss point, so that

$$\Delta t_{max} \leq \tau \left(\frac{\bar{\varepsilon}}{\dot{\bar{\varepsilon}}_c} \right), \tag{1}$$

where $\bar{\varepsilon}$ is the total effective strain and $\dot{\bar{\varepsilon}}_c$ is the effective creep strain rate. Another useful limit can be imposed to avoid oscillatory solutions which often occur if the time step changes too abruptly,

$$\Delta t_{max} \leq k \Delta t_{old}, \tag{2}$$

where k is a specified constant and Δt_{old} is the previous time step length. The third limit on the time step requires that a minimum number of time steps be completed during the release of a node according to

$$\Delta t_{max} \leq \frac{t_{end} - t_{start}}{N + M}, \tag{3}$$

where N and M are guesses for the number of displacement increments and load decrements, respectively, and t_{start} and t_{end} are the times at which release of the current crack tip node begins and ends, respectively.

After choosing the minimum of the Δt_{max} values in (1)-(3) above, the displacement increment or load decrement is computed based on this time step. Displacements are prescribed until the remaining reaction at the crack tip node is less than ten percent of the initial reaction ***OR*** until a specified amount of time (t_{switch}) has elapsed:

$$t_{switch} = (t_{end} - t_{start}) \left(\frac{N}{N + M} \right). \tag{4}$$

Here, t_{switch} is the maximum period of time during which displacements are incremented. Displacement increments are given as

$$\Delta V = V_{ref} \left(\frac{\Delta t}{t_{switch}} \right), \tag{5}$$

where V_{ref} is the y-displacement at the node behind the crack tip at $t=t_{start}$. When the reaction at the node has been reduced to ten percent of its initial value or the y-displacement at the crack tip node is equal to V_{ref}, the remaining load on the node is reduced to zero over two or more time steps. The load decrements at the crack tip, denoted as ΔR_y, are given by

$$\Delta R_y = -R_y \left(\frac{\Delta t}{t_{end} - t + \Delta t} \right), \tag{6}$$

where R_y is the ***remaining*** nodal reaction. When $t=t_{end}$, (13) shows that the remaining nodal force is reduced to zero since $\Delta R_y=-R_y$.

This variable time-step, nodal release algorithm performed very effectively for the creep-brittle materials studied, resulting in time steps ranging from 10^{-17} to 10^{-1} hours. The number of time steps required to completely release the crack tip nodes varied from around 250 for the first node to 50 for other nodes. The user defined time step controlling parameters were chosen as $\tau=0.04$ and $k=1.35$. Values of N and M were chosen as 10 and 2, respectively for all releases. The relative magnitudes of N and M are important, as seen in (4), while the absolute magnitudes have little effect on the overall performance since the maximum time step given by (1) or (2) usually governs the time stepping process. However, selection of N and M values that are too small could result in accuracy and stability problems, while values of N and M that are too large could result in unnecessary computational effort.

Implementation

Here, we present an example of the types of analyses conducted on several creep-brittle materials. Experimentally observed crack growth histories of four aluminum alloy 2519-T87 compact tension specimens were numerically enforced to study the evolution of crack tip fields and far-field fracture parameters (a similar approach was taken by Bassani, et al. [8]). Details of the implementation for specimen BCH-6 are provided below.

The time-dependent deformation characteristics for the Aluminum Alloy 2519-T87 are accurately described by the following constitutive law:

$$\dot{\epsilon} = \frac{\dot{\sigma}}{E} + c(\sigma)^N(\epsilon_{pc})^{-p} + A_1(\sigma)^{n_1} + A_2(\sigma)^{n_2} \quad . \tag{7}$$

Here, σ is stress, ϵ_{pc} is the primary creep strain, and c, N, p, A_1, n_1, A_2 and n_2 are creep constants. This constitutive model was incorporated into the finite element code and used to model the response of each fracture specimen.

A constant external load of 10.5 kN was applied to specimen BCH-6 with width and thickness of 5.08 cm and 2.21 cm, respectively. The specimen was side grooved 10 percent on each side (the thickness at the side grooves was 1.77 cm) so that plane strain fracture conditions were assumed to apply. Crack growth began at a crack length of 2.25 cm and ended 105 hours later at a crack length of 2.52 cm (unstable fracture occurred at the final crack length). A plot of the crack growth history (Fig. 12) reveals a relatively long incubation period followed by rapid crack growth.

The finite element mesh used to model specimen BCH-6 consists of 1142 four noded linear isoparametric elements (Fig. 13). Crack growth is simulated by releasing a sequence

of 40 nodes along the lower boundary of the dense portion of the mesh. Crack growth begins six elements to the right of the start of the small square elements and ends six element to the left of the end of the small square elements. The crack growth increment is 67.3 μm which is smaller than the estimated average grain size of 100μm. The release time of each of the 40 nodes along the crack growth path is estimated using a smooth fit of the experimentally observed crack length versus time history (Fig. 12).

Numerical Results for Aluminum Alloy 2519-T87

Evolution of Crack Tip Fields

- For creep-brittle materials, the rate of expansion of the creep zone is comparable to the rate of crack growth resulting in a creep zone that is confined to a thin strip of material adjacent to the crack growth path. Using a visualization program developed as part of this work, contour plots of creep strains at three times during crack growth are shown Figure 14. Here, the red regions represent effective creep strains in excess of 0.005, while the blue regions denote near zero (negligible) creep strains.

- Profiles of effective stress along a radial line from the crack tip at $\theta=90^\circ$ reveal that stresses in a region outside the creep zone scale with $r^{-1/2}$ throughout the crack growth history (Fig. 15). Consequently, small-scale creep conditions exist and K describes the crack tip fields in an annular region around the crack tip.

- Following an initial transient period, the creep zone for specimen BCH-6 expands in a roughly "self-similar" fashion, as demonstrated by ratios of the creep zone radius along $\theta=90^\circ$ to that along $\theta=0^\circ$ (Fig. 16).

Correlation of Crack Growth with Fracture Parameters

- Creep-ductile conditions exist when the deflection at the load line is dominated by creep deformation so that $\dot{V}_c/\dot{V}\geq 0.8$ [9], where $\dot{V}_c$ is the creep component of the load line deflection rate and $\dot{V}$ is the total load line deflection rate. According to this criterion, crack growth in specimen BCH-6 does not occur under creep-ductile conditions (Fig. 17). In fact, negative deflection rate ratios exist in the initial stages of crack growth, indicating highly creep-brittle crack growth conditions.

- The applicability of small-scale creep conditions coupled with the existence of similitude provides hope that the later stages of crack growth can be correlated with K. Figure 18 reveals good correlation of K with crack growth rates after the initial period of transience for the thicker specimens. Crack growth rates also have a power-law dependence on K for the thinner specimen, although the dependence is shifted relative to the thicker specimens. The ability of the thinner specimen to tolerate higher K levels is attributed to reduced constraint, since it is believed that crack tip damage processes accelerate under increasing triaxiality levels, particularly for creep-brittle materials.

- Although experimental evidence discourages application of C_t to creep-brittle fracture, the numerical results indicate excellent correlation of C_t with crack growth rates (Fig. 19) for positive load line deflection rates due to creep ($\dot{V}_c>0$).

Assessment of Accuracy

- Accuracy of the numerical results were verified by comparison with ABAQUS, a commercial finite element code which allows for nodal release [10]. Discrepancies in computed load line deflections were well within one percent for creep-brittle crack growth in a material deforming according to an elastic-power-law creep constitutive relation.

- Comparison of numerical and experimental load line deflections in Figure 20 reveals similar overall trends with some deviation near the end of the test.

Partitioning of Load Line Deflection

Load line deflection measurements are typically employed to compute a variety of far field fracture parameters, indirectly suggesting that these deflection measurements are somehow directly related to the fracture process. Therefore, a good understanding of the relation of the evolving crack tip fields to load line deflection measurements for creep-brittle and creep-ductile materials is desirable. Some key results of a set of growing crack finite element analyses in which constant crack growth rates were enforced are given below:

- For creep-ductile crack growth, the full effect of previously accumulated creep deformation on the load line deflection due to creep (V_c) remains intact as subsequent crack growth occurs. Thus, $\dot{V}_c$ is related to the current rate of accumulation of creep deformation and not to history effects (effects of previously accumulated creep deformation on the load line deflection rate).

- For creep-brittle crack growth, the effect of previously accumulated creep deformation on V_c diminishes as residual creep deformation is left in the wake of the growing crack. Consequently, the load-line deflection rate due to creep ($\dot{V}_c$) is related to both the current rate of expansion of the creep zone and to the residual creep deformation left in the wake of the growing crack. The diminishing effect of residual creep deformation produces a negative contribution to $\dot{V}_c$, suggesting that negative values of $\dot{V}_c/\dot{V}$ are possible, depending on competing effects of history and the instantaneous rate of accumulation of creep deformation near the tip.

- The existence of small-scale creep conditions throughout the crack growth history coupled with the diminishing effect of creep deformation left in the wake of crack growth permits continued applicability of an Irwin type creep zone correction throughout the crack growth history. That is, the expression

$$V_c = \frac{2BK^2(1-\nu^2)}{PE}\,\beta r_c \qquad (8)$$

is valid under small-scale creep conditions, where ß maintains a value of approximately 1/3 as for a stationary crack.

- The differences in the relation of V_c to the evolving crack tip fields demonstrate that the physical interpretation of fracture parameters based on $\dot{V}_c$, such as C_t, is somewhat different for creep-ductile and creep-brittle materials.

Re-interpretation of Time-Dependent Fracture Parameters

Crack growth correlations based exclusively on K are effective for aluminum 2519-T87 under small-scale creep conditions in which similitude roughly exists. However, transient regimes of crack growth are not adequately modeled by K, which is a time and history independent function of loading, crack length and geometry. In the interest of incorporating time or history into a far-field measure of the severity of crack tip conditions, time-dependent fracture parameters based on stationary crack analyses (applicable to creep-ductile crack growth) may be re-interpreted for growing cracks under small-scale yielding (applicable to creep-brittle crack growth). Important aspects of this re-interpretation are given below.

- The creep zone is chosen as the basis for re-interpretation of the time dependent fracture parameters C_t and C(t). Here, the rate of expansion of the creep zone ($\dot{r}_c$) is defined as the creep zone expansion rate that would be experienced at the tip of a stationary crack with a creep zone size equal to that of the growing crack. This definition removes the negative contribution of history effects on $\dot{V}_c$, resulting in $\dot{V}_c$ values that are always greater than or equal to zero.

- Correlation of fracture based on C_t and C(t) for growing cracks can be generalized as correlations between crack growth rates and K/r_c^q, where q is an exponent chosen to provide the best overall correlation. Using this approach, improved correlation under transient conditions results (Fig. 21). Again, note that the data which are not well-correlated were obtained from a thin specimen.

Impact of Numerical Results on Methods of Experimental Analysis

Inherent problems exist in experimental determination of time-dependent fracture parameters for creep-brittle materials. Evidence of these problems is highlighted by conflicting reports from experimental and numerical analyses concerning correlation of crack growth rates with C_t. The root of the problem lies in the inability to experimentally resolve accurate values of $\dot{V}_c$ when $\dot{V}_c/\dot{V}$ ratios are very small (Fig. 17). Small $\dot{V}_c/\dot{V}$ ratios coupled

with limited accuracy in determining crack lengths and corresponding crack growth rates result in inaccurate values of $\dot{V}_c$, since $\dot{V}_c=\dot{V}-\dot{V}_c$ and $\dot{V}_e$ depends on measured $\dot{a}$ values. These inaccurate $\dot{V}_c$ values translate into inaccurate C_t values which understandably exhibit little or no correlation with $\dot{a}$. Experimentally based crack growth correlations based on K/r_c^q suffer from similar problems. However, these problems can be overcome by coupling experimental and numerical approaches to creep-brittle crack growth, as demonstrated by this research.

PROGRAM DELIVERABLES

This program has produced significant results, both in terms of scholarly findings in publications and in terms of education of graduate students.

Papers Completed:

1. A. Saxena and K. A. Jones, "Creep Crack Growth in Rapidly Solidified Aluminum Alloy 8009", in Aluminum Alloys - Their Physical and Mechanical Properties, Vol. I - Proceedings of the 4th International Conference, Sept. 11-16, 1994, Atlanta, GA, pp. 757-764.

2. P. S. Grover and A. Saxena, "Developments in Elevated Temperature Crack Growth Testing and Data Analysis," ECF-10, 1994, pp. 1-20.

3. Hall, D. E., McDowell, D.L. and Saxena, A., "Numerical Analysis of Crack Growth in Creep-Brittle Aluminum Alloy 8009," 1995 NSF Design, Manufacturing and Industrial Grantees Meeting, Institute for Mechanics and Materials, La Jolla, California, January 4-6, 1995.

4. Hall, D. E., McDowell, D.L. and Saxena, A., "Some Aspects of Crack Growth in Creep Brittle Materials," Submitted to the International Symposium for Inelastic Deformation, Damage and Life Analysis, Honolulu, Hawaii, July 30-August 3, 1995.

Papers in Progress:

5. Hamilton, B.C., Hall, D.E., Saxena, A. and McDowell, D., "Creep Crack Growth Behavior of Aluminum Alloy 2519: Part I - Experimental Analysis," to be presented at the 27th National Symposium on Fatigue and Fracture Mechanics, June 26-29, 1995, Williamsburg, VA and submitted for publication in an ASTM STP.

6. Hall, D.E., Hamilton, B.C., McDowell, D. and Saxena, A, "Creep Crack Growth Behavior of Aluminum Alloy 2519: Part II - Numerical Analysis," to be presented at the 27th National Symposium on Fatigue and Fracture Mechanics, June 26-29, 1995, Williamsburg, VA and submitted for publication in an ASTM STP.

7. A. Saxena, K. A. Jones, D. Hall and D. L. McDowell, "Crack Growth in Creep-Brittle Materials," manuscript under preparation for submission to Materials and Metallurgical Transactions, June 1995.

8. Fan Yang and A. Saxena, "Fracture Propagation in Uniaxial SiC/Si_cN_4 Composite," to be presented at the 27th National Symposium on Fatigue and Fracture Mechanics, June 26-29, 1995, Williamsburg, VA and submitted for publication in an ASTM STP.

9. Hall, D., McDowell, D.L. and Saxena, A., "Numerical Studies of Crack Growth in Creep-Brittle Materials," manuscript under preparation for submission to Intnational Journal of Fracture.

Presentations:

1. A. Saxena and K. A. Jones, "Creep Crack Growth in Rapidly Solidified Aluminum Alloy 8009," Fourth International Conference on Aluminum Alloys, Sept. 11-16, 1994 Atlanta, Ga.

2. P. S. Grover and A. Saxena (invited keynote) Developments in Elevated Temperature Crack Growth Testing and Data Analysis," Tenth European Conference on Fracture, ECF-10, Berlin, Sept. 19-24, 1994.

3. A. Saxena, "Crack Growth in Creep-Brittle Materials," TMS Symposium on Elevated Temperature Behavior of Advanced Materials, Oct. 6 - 10, 1994, Chicago, Il.

4. A. Saxena and D. L. McDowell (invited), "Crack Growth in Creep-Brittle Materials," NSF Workshop on Mechanics and Processing Interface, Oct. 24 - 26, 1994, Lake Lanier Island, Ga.

5. Fan Yang and A. Saxena, "Fracture Propagation in Uniaxial SiC/Si_3N_4 Composite," to be presented at the 27th National Symposium on Fatigue and Fracture Mechanics, Williamsburg, Va, June 1995.

6. Hamilton, B.C., Hall, D.E., Saxena, A. and McDowell, D., "Creep Crack Growth Behavior of Aluminum Alloy 2519: Part I - Experimental Analysis," to be presented at the 27th National Symposium on Fatigue and Fracture Mechanics, June 26-29, 1995, Williamsburg, VA and submitted for publication in an ASTM STP.

7. Hall, D.E., Hamilton, B.C., McDowell, D. and Saxena, A, "Creep Crack Growth Behavior of Aluminum Alloy 2519: Part II - Numerical Analysis," to be presented at the 27th National Symposium on Fatigue and Fracture Mechanics, June 26-29, 1995, Williamsburg, VA and submitted for publication in an ASTM STP.

Students Supported:

Ms. Kimberly A. Jones (joint Georgia Tech/NSF support), M.S. 1993, thesis topic: "The Creep Behavior of Aluminum Alloy 8009," current affiliation: Textron Co., Memphis, Tn.

Ms. Fan Yang (Ph.D. student, joint Georgia Tech/NSF support), thesis topic: "Creep Behavior of Nicalon fiber SiC reaction bonded Si_3N_4 Composite," expected graduation date 12/95.

Mr. David E. Hall (Ph.D. student, NSF support), thesis topic: "Numerical Studies of Crack Growth in Creep Brittle Materials," expected graduation date 8/95.

References

[1] Dogan, B., Saxena, A., and Schwalbe, K.-H., "Creep Crack Growth in Creep-Brittle Ti-6242 Alloys," Materials at High Temperatures, Vol. 10, No. 2, 1992, pp. 138-143.

[2] Gill, Y., "Creep Crack Growth Characterization of SA-106 C Carbon Steel," Ph.D. Thesis, Materials Science and Engineering, Georgia Institute of Technology, Atlanta, Georgia, March 1994.

[3] Jones, K. A., "The Creep Behavior of Aluminum Alloy 8009," Master's Thesis, Materials Science and Engineering, Georgia Institute of Technology, Atlanta, Georgia, September, 1993.

[4] Leng, Y., Porr, W. C.,Jr., and Gangloff, R.P., "Time Dependent Crack Growth in P/M Al-Fe-V-Si at Elevated Temperatures," Scripta Metallurgica et Materialia, Vol .25, 1991, pp.895-900.

[5] Leung, C.-P., McDowell, D. L., and Saxena, A., "Inclusion of Primary Creep in the Estimation of the C_t Parameter," International Journal of Fracture, Vol. 46, 1990, pp. 81-104.

[6] Hawk, D. E. and Bassani, J. L., "Transient Crack Growth Under Creep Conditions," J. Mech. Phys. Solids, Vol. 34, No. 3, 1986, pp. 191-212.

[7] Moyer, T. E., and Liebowitz, H., "Creep Crack Growth Modeling and Near Tip Stress Fields," Engineering Fracture Mechanics, Vol. 28, No. 5/6, 1987, pp. 601-621.

[8] Bassani, J. L., Hawk, D. E., and Saxena, A., "Evaluation of the C_t Parameter for Characterizing Creep Crack Growth Rate in the Transient Regime," ASTM STP 995, American Society for Testing and Materials, Philadelphia, 1989, pp. 7-26.

[9] Saxena, A. and Landes, J. D., "Characterization of Creep Crack Growth in Metals," Advances in Fracture Research, 6th International Conference on Fracture, Pergamon Press, 1984, pp. 3977-3988.

[10] Hibbitt, Karlsson, & Sorensen, Inc., ABAQUS, Version 5.2, 1994.

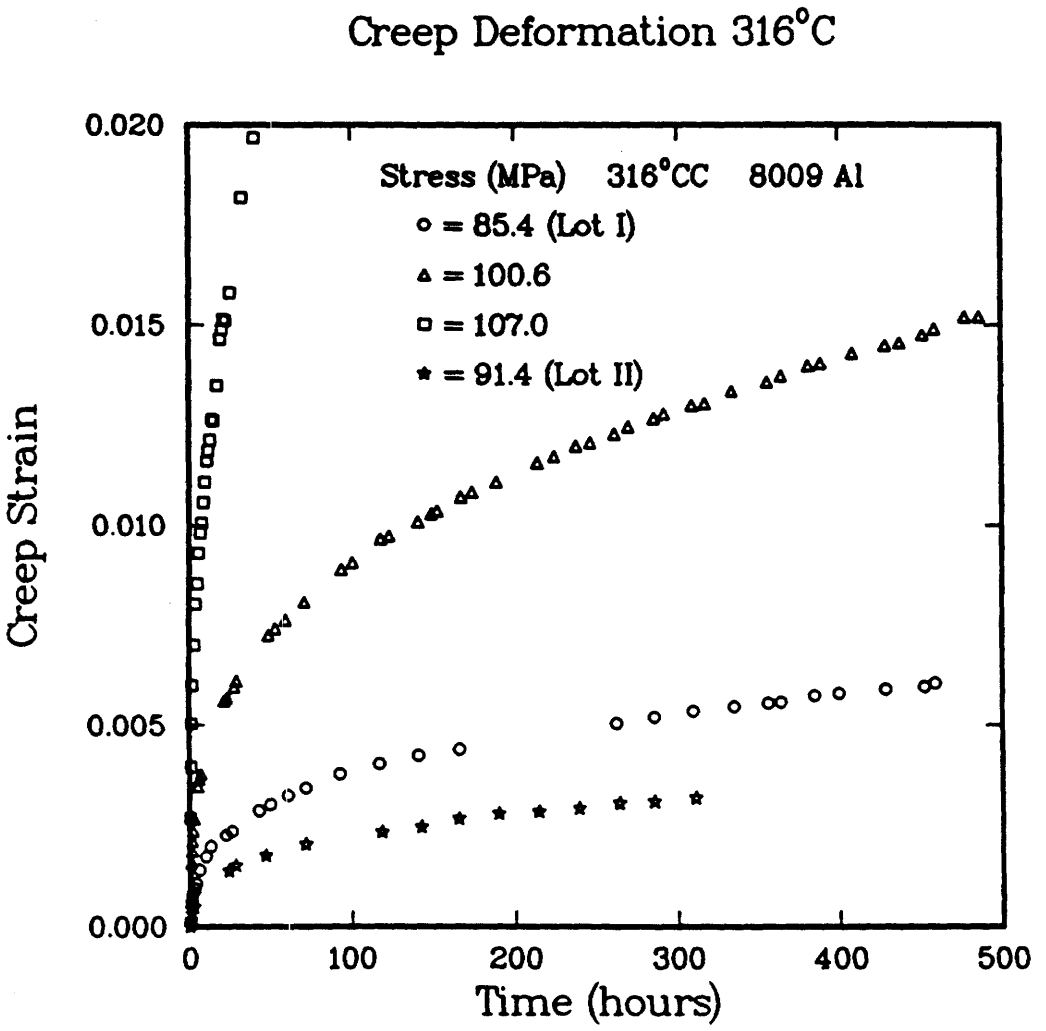

Figure 1 - Creep strain as a function of time for Al alloy 8009 at 316°C at different stress levels.

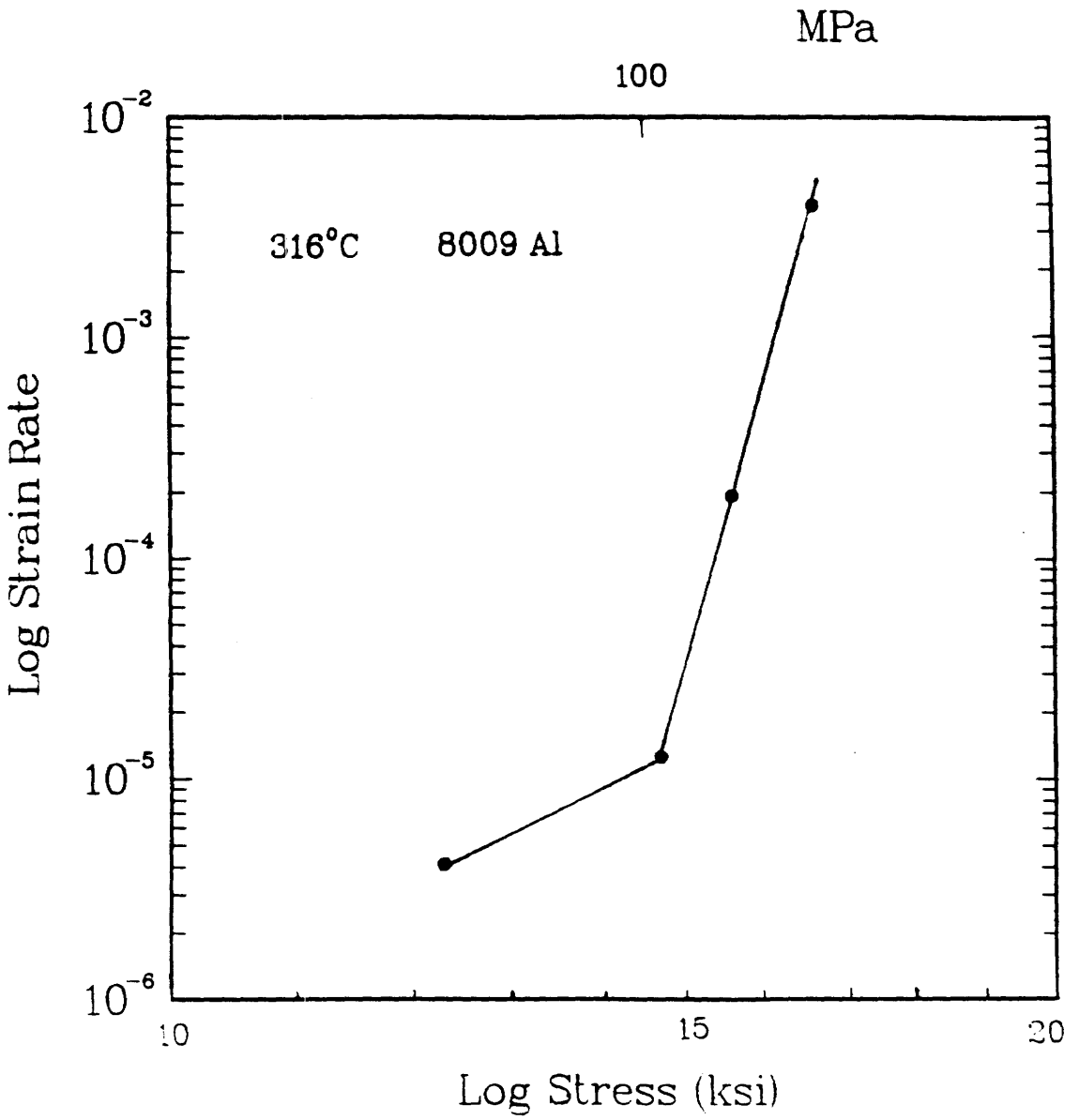

Figure 2 - Steady-state creep rate as a function of stress for Al alloy 8009 at 316°C.

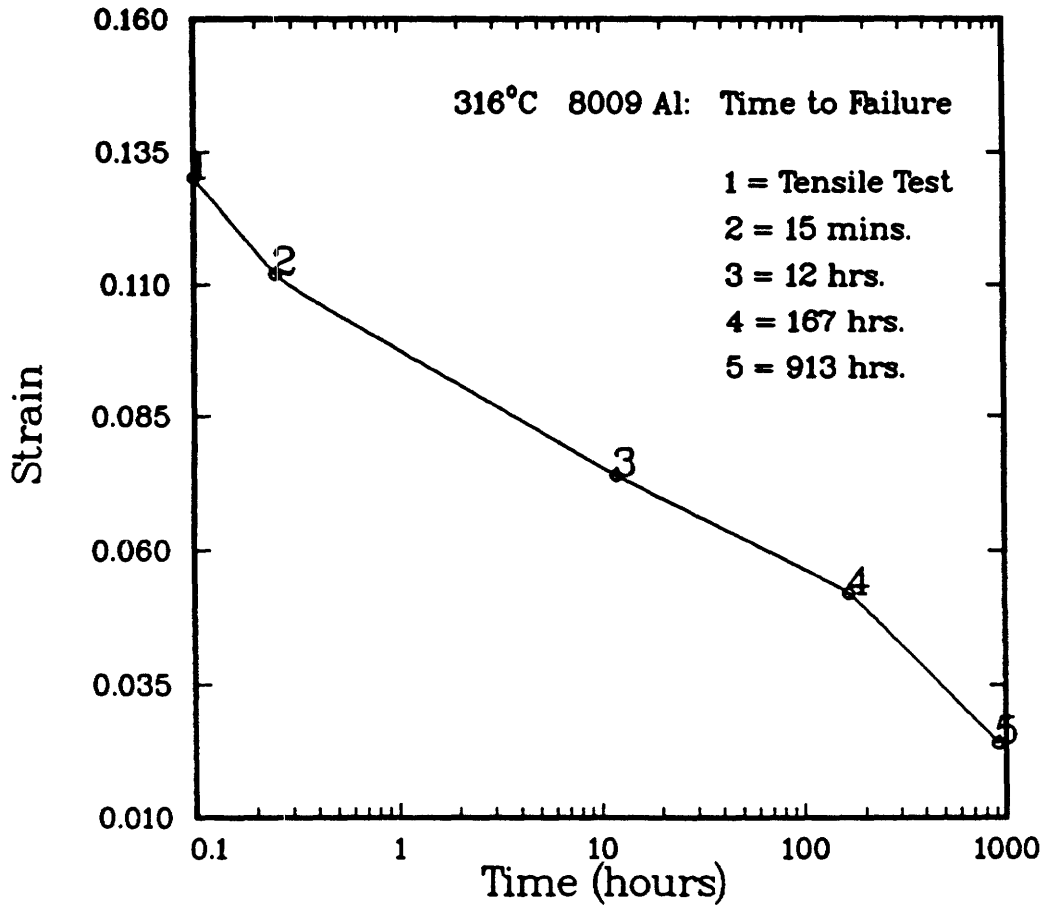

Figure 3 - Rupture ductility as a function of test duration of creep tests for Al alloy 8009 at 316°C.

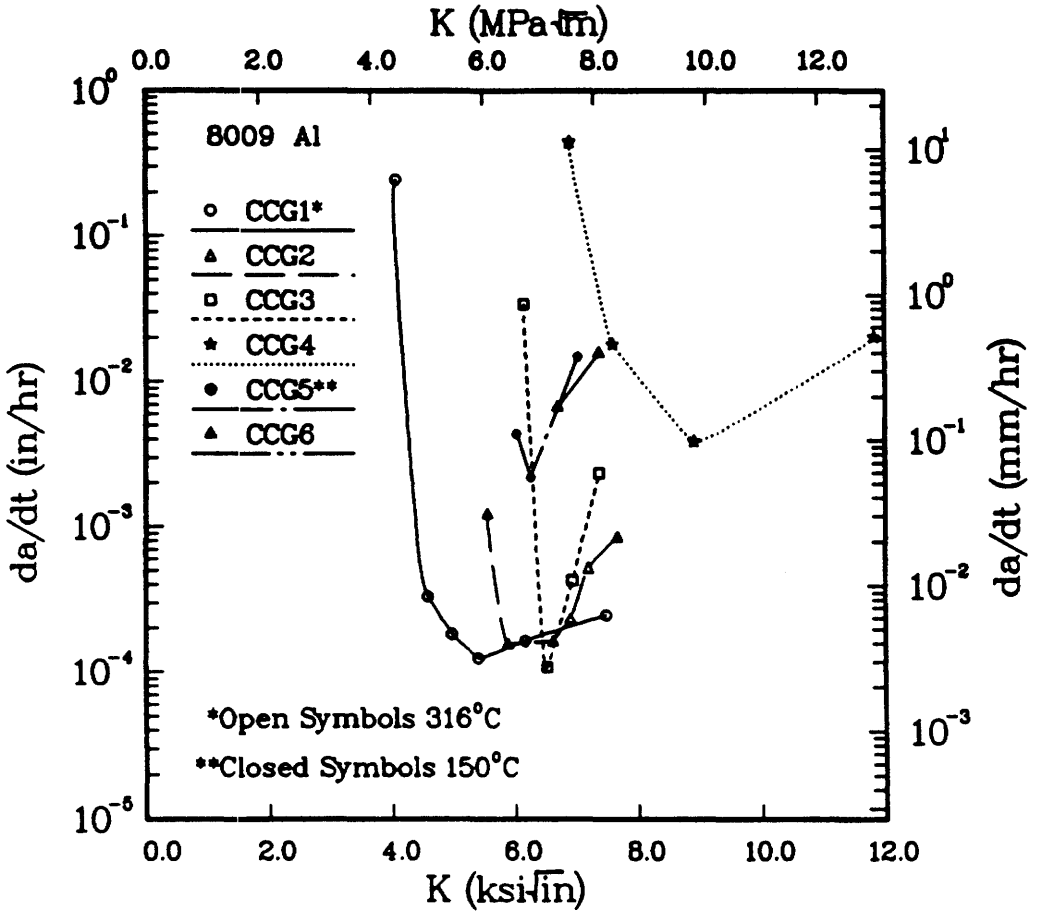

Figure 4 - Creep crack growth rate of Al alloy 8009 as a function of stress intensity parameter, K.

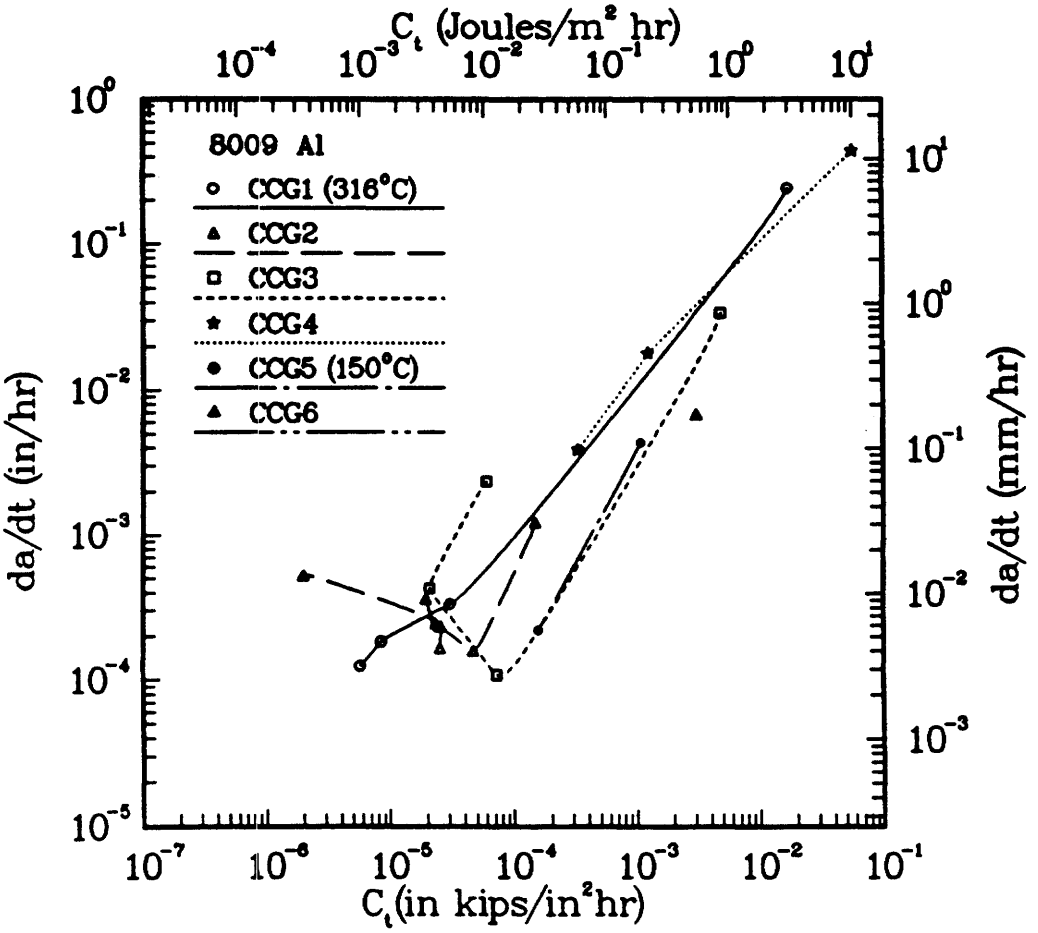

Figure 5 - Creep crack growth rate of Al alloy 8009 as a function of C_t.

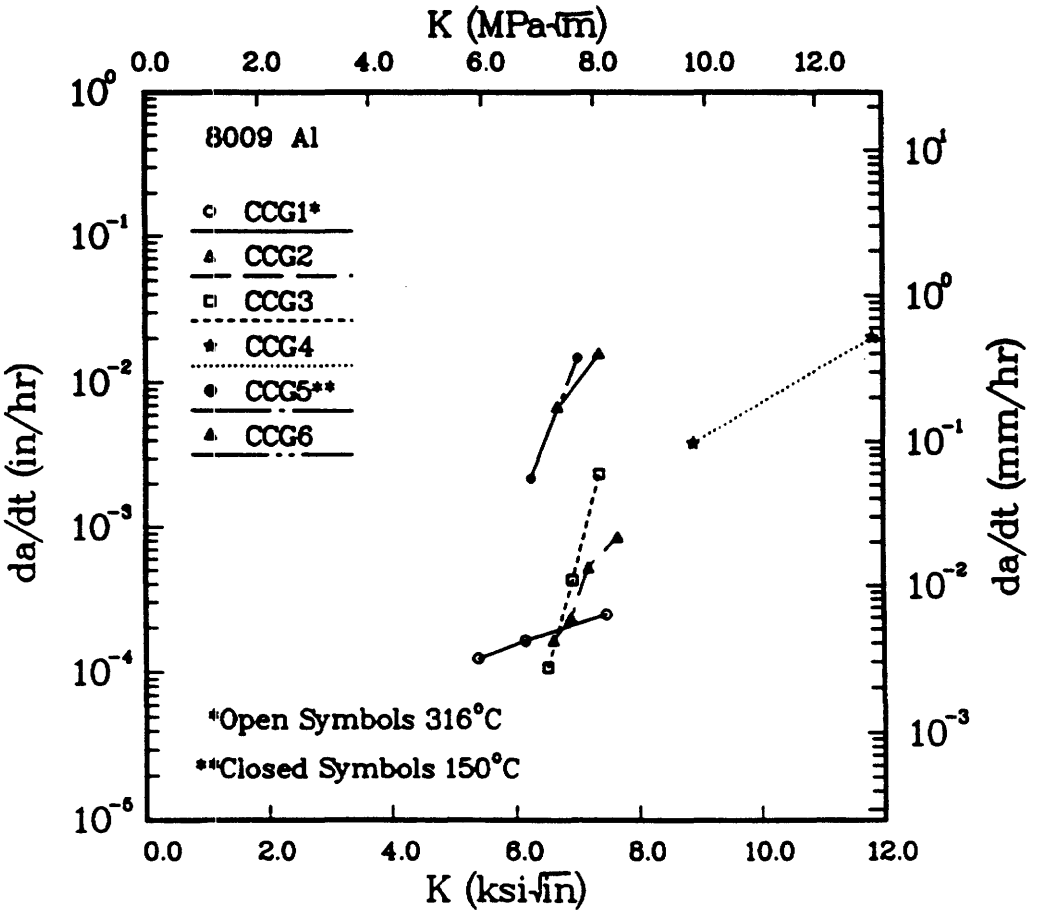

Figure 6 - Plot of creep crack growth rate as a function of K from the increasing da/dt portion of the tests for Al alloy 8009.

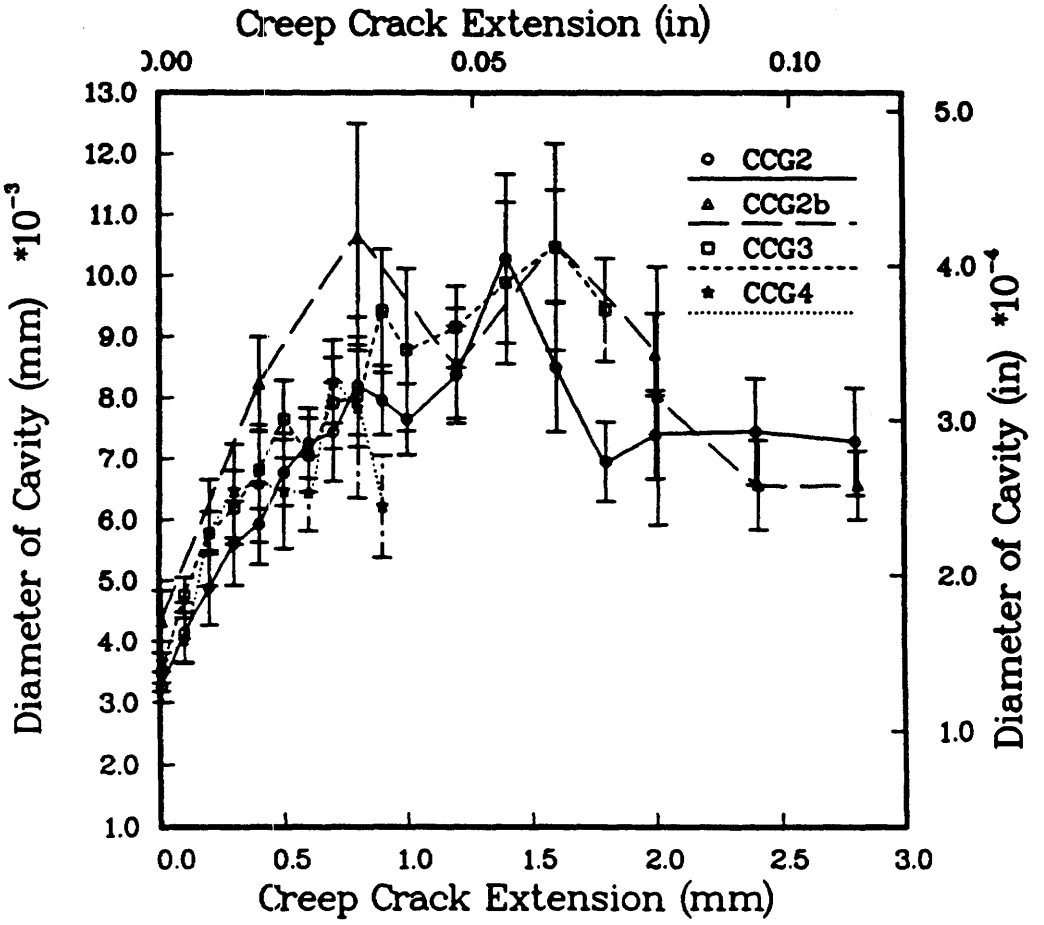

Figure 7 - Creep cavity diameter as a function of creep crack extension during various tests for Al alloy 8009.

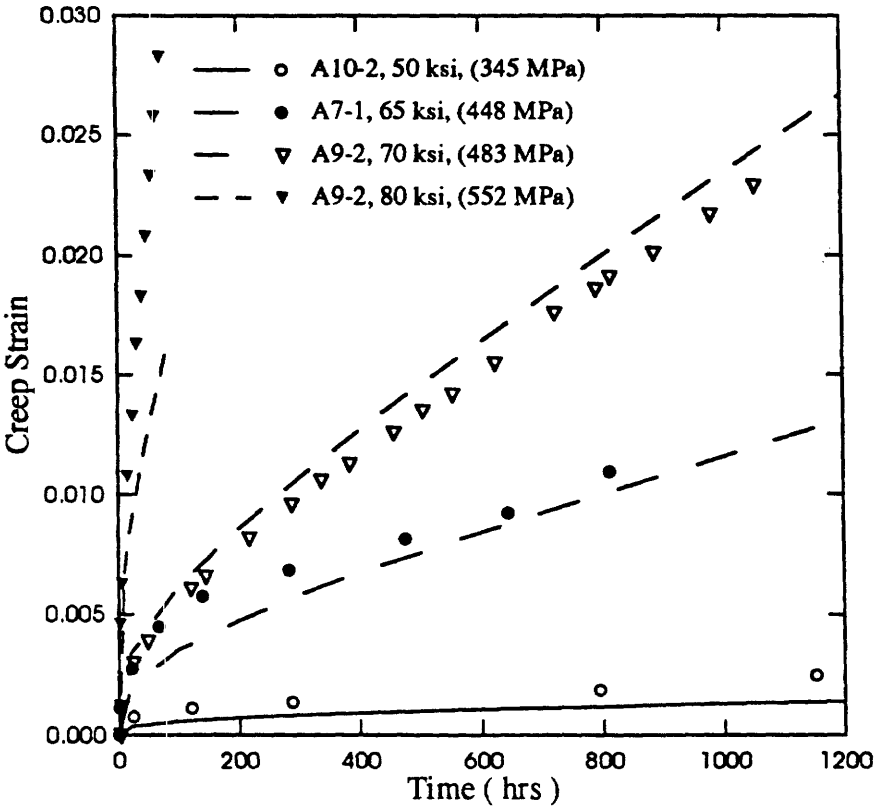

Figure 8 - Creep deformation as a function of time at various stress levels for aged C-Mn steel at 360°C.

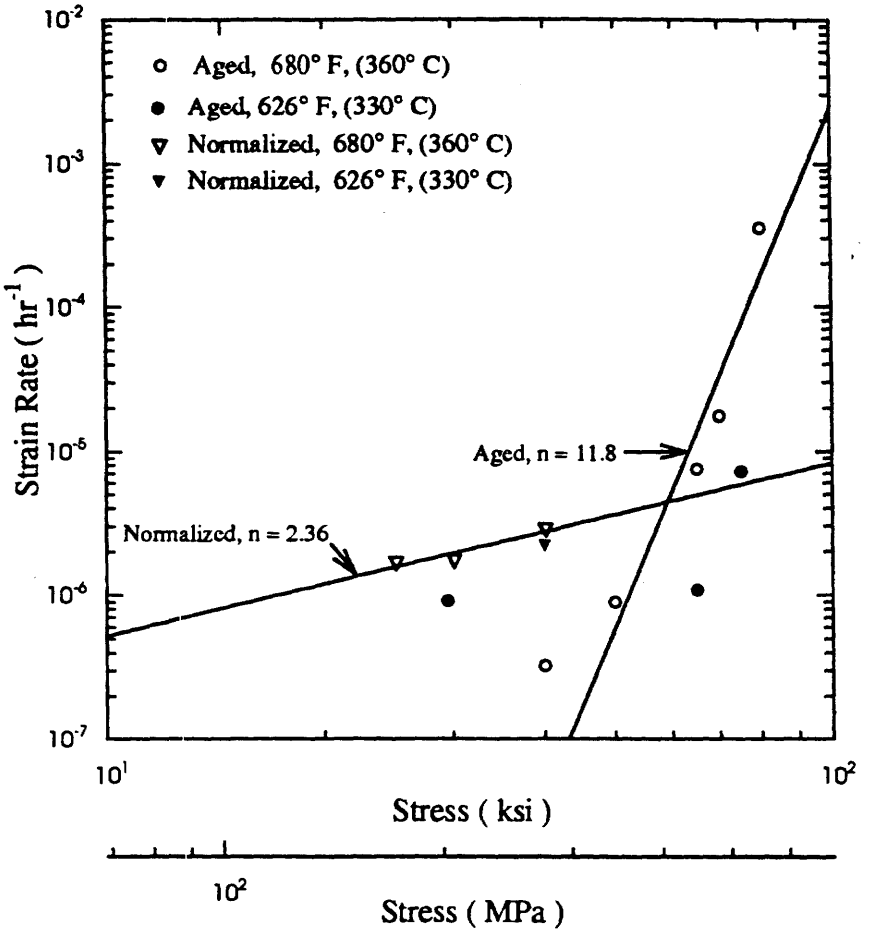

Figure 9 - Steady-state creep strain rate as a function of stress for C-Mn Steel.

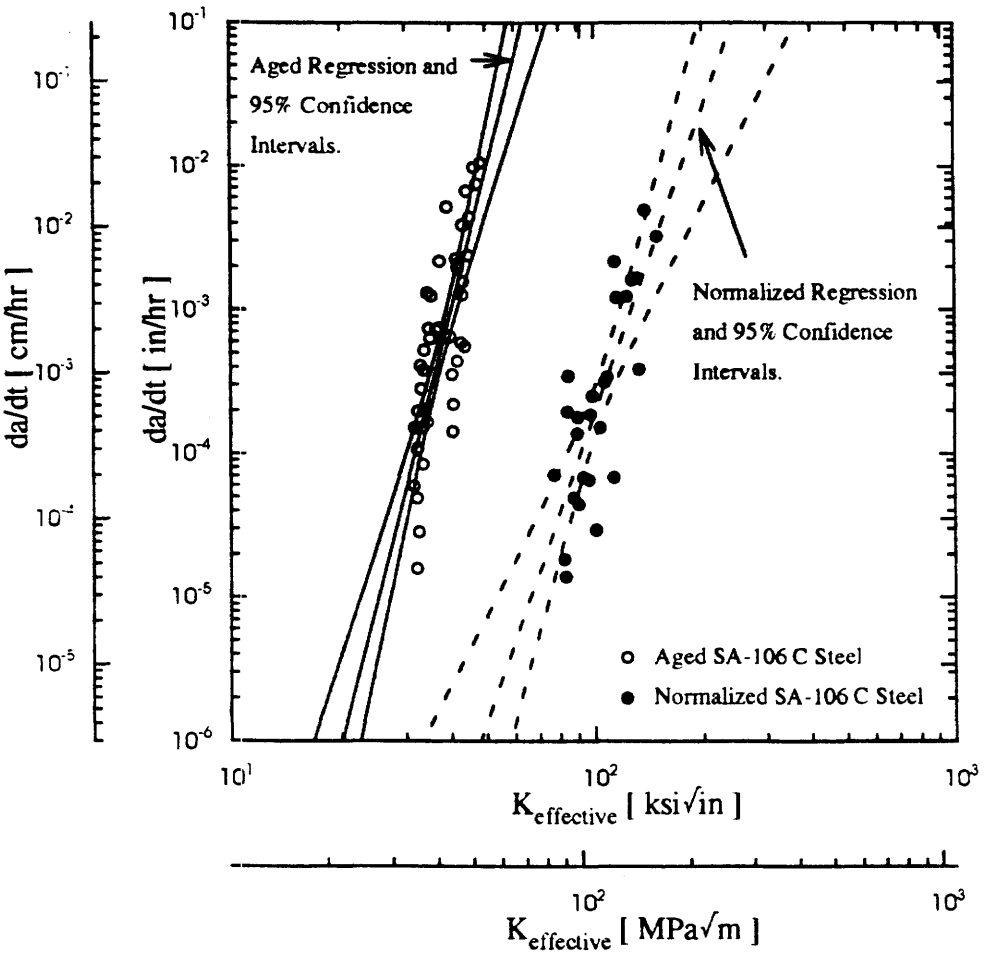

Figure 10 - Creep crack growth rate as a function of K for C-Mn Steel.

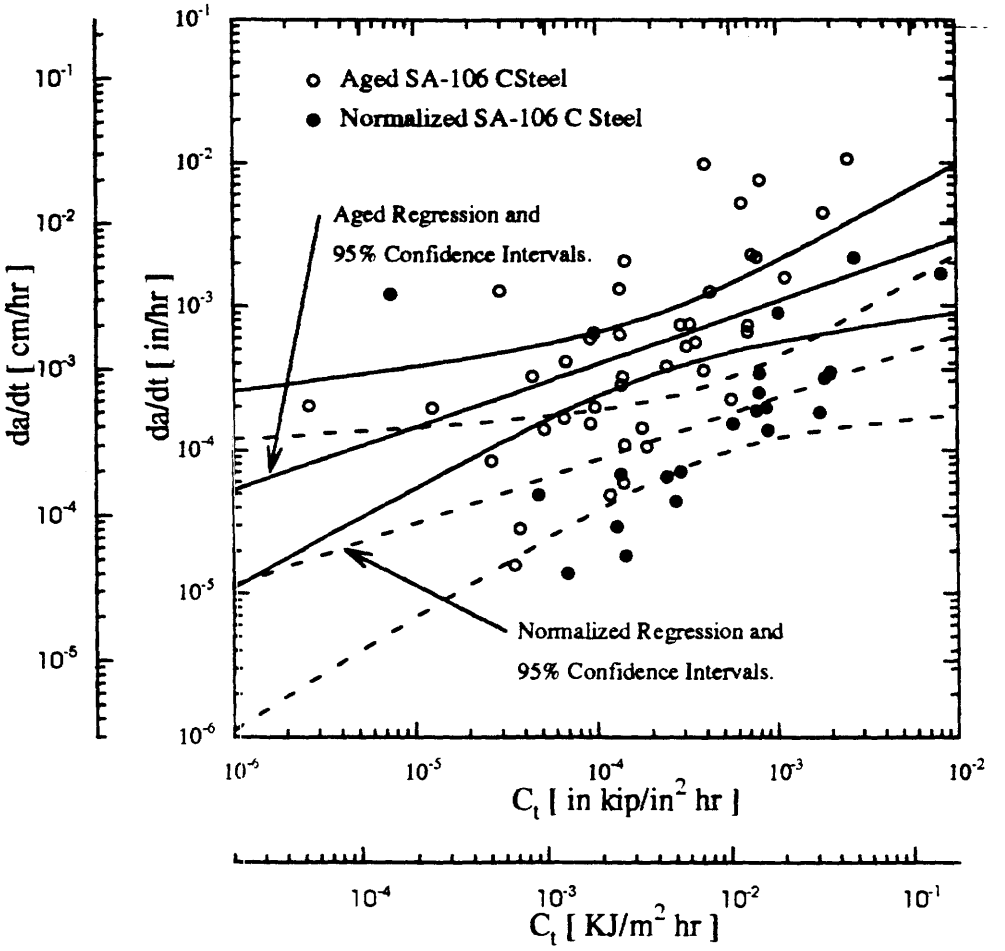

Figure 11 - Creep crack growth rate as a function of C_t for C-Mn Steel.

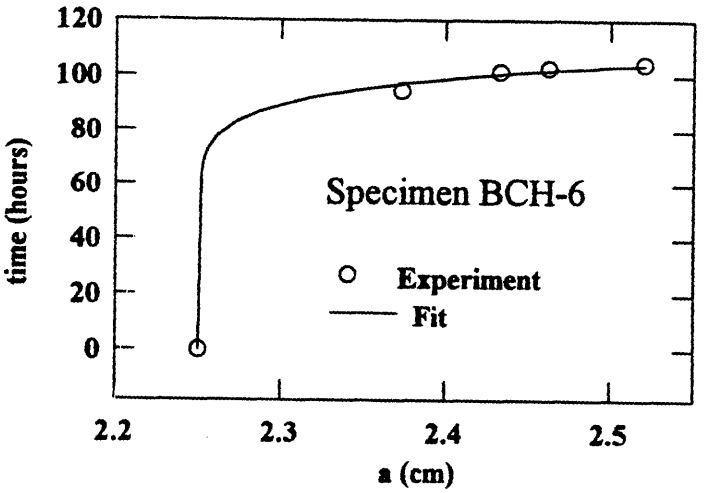

Figure 12 - Experimentally determined crack growth history along with curvefit.

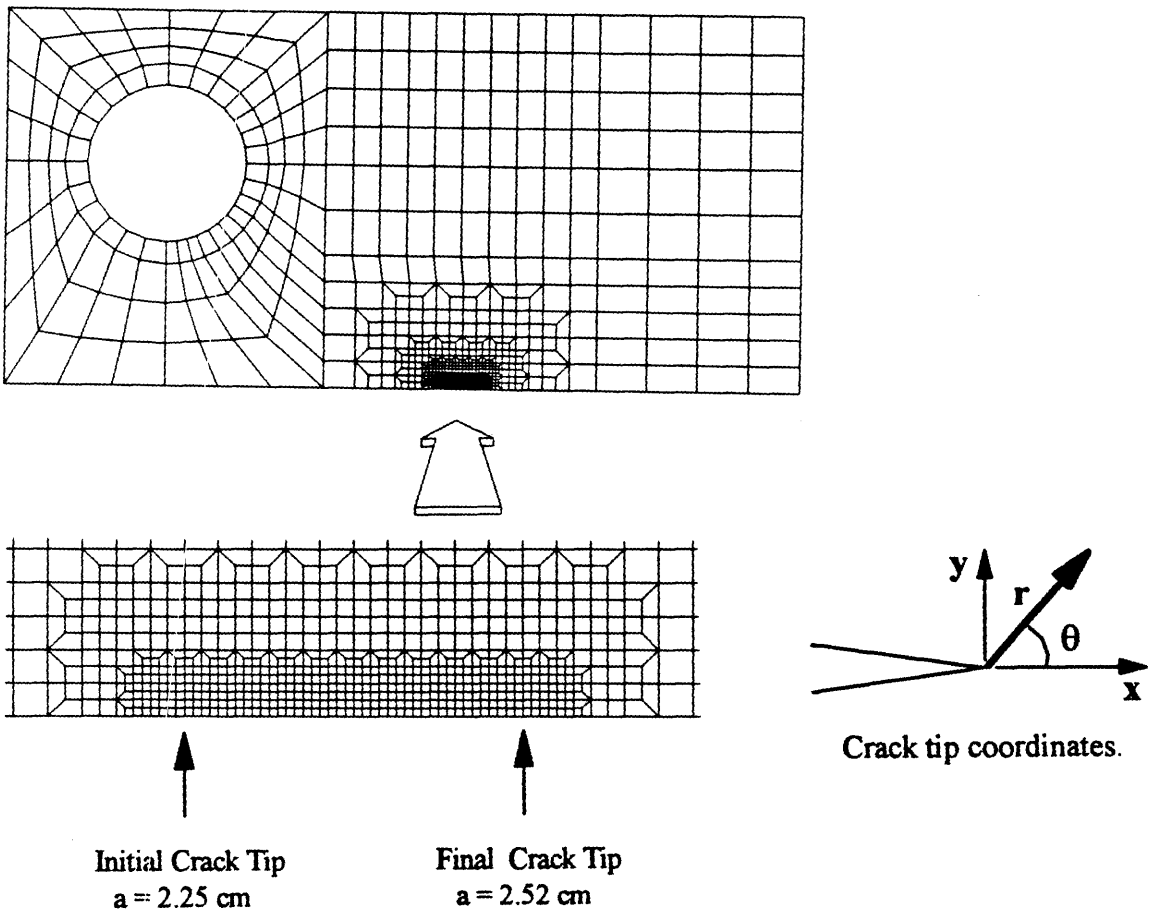

Figure 13 - Finite element mesh for specimen BCH-6.

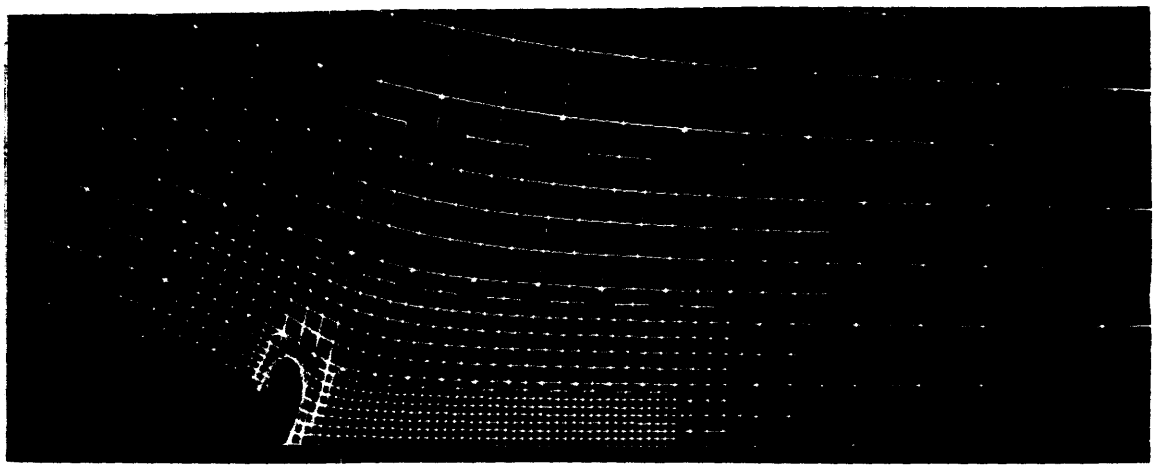

Time = 74.53 hours; Crack Length = 2.26 cm

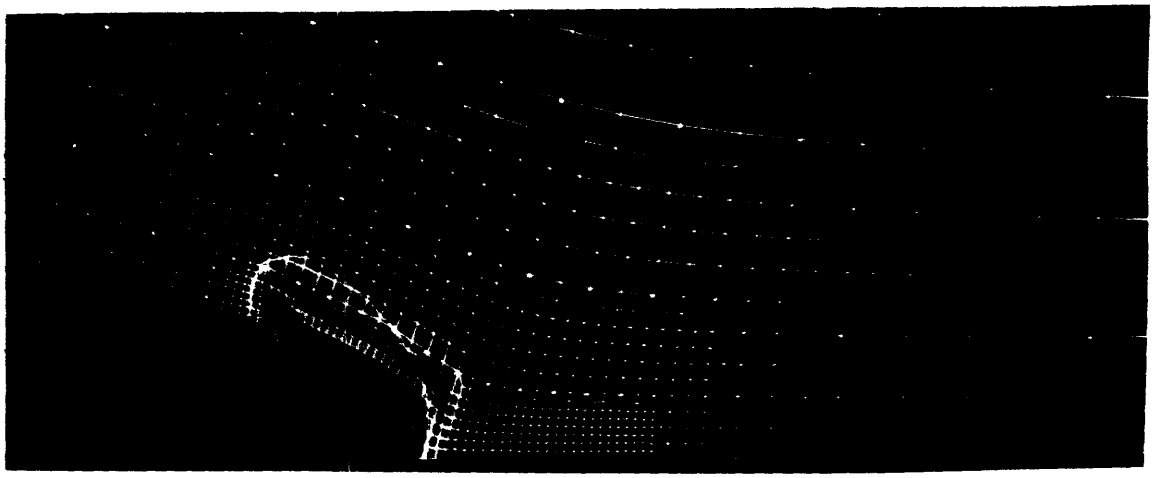

Time = 98 hours; Crack Length = 2.39 cm

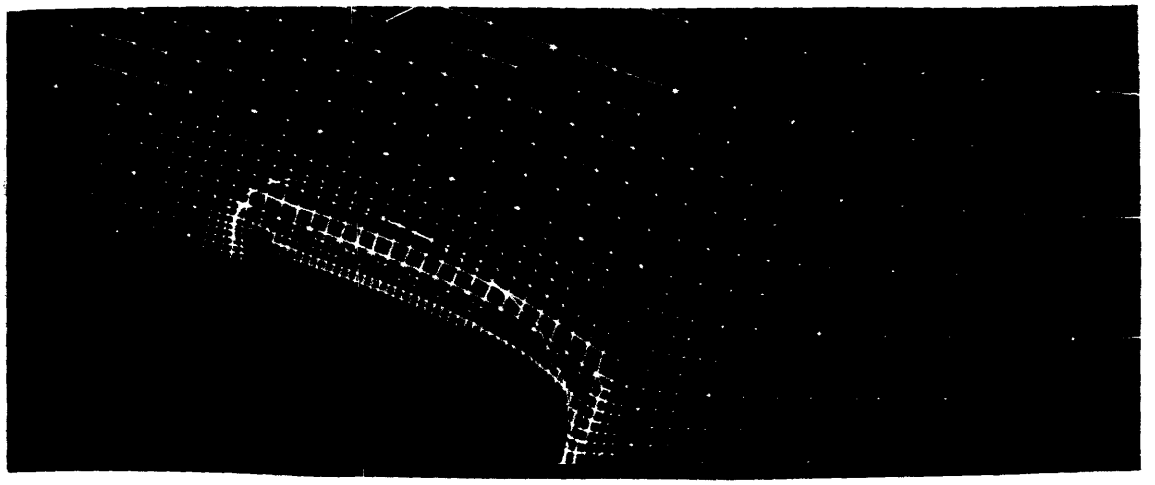

Time = 104 hours; Crack Length = 2.52 cm

Figure 14 - Contour plots of effective creep strain at various stages of growth.

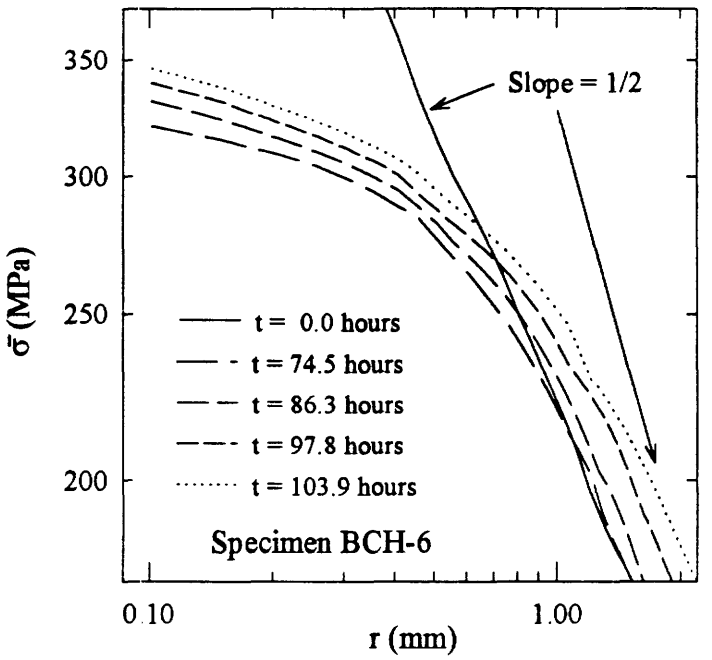

Figure 15 - Profiles of effective stress along $\theta = 90^{\circ}$.

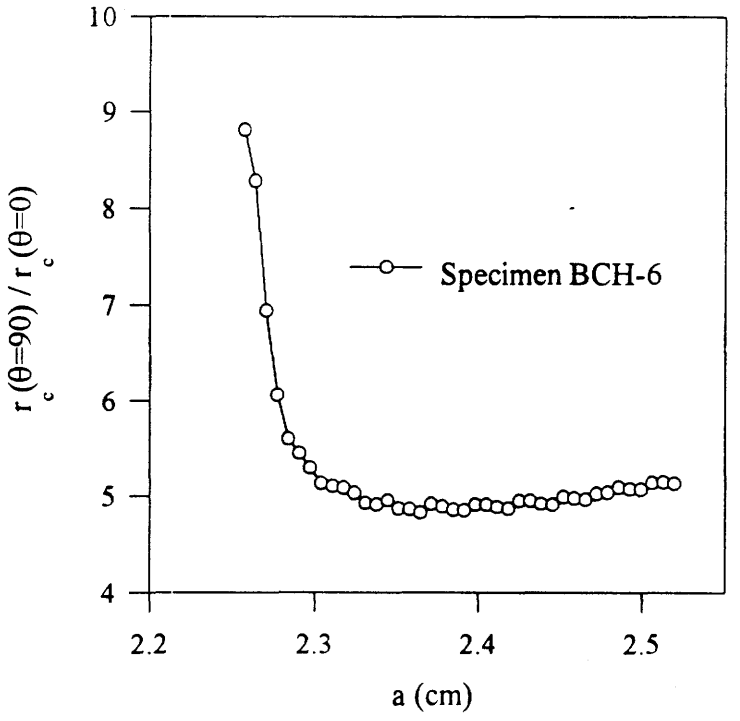

Figure 16 - Check of similitude.

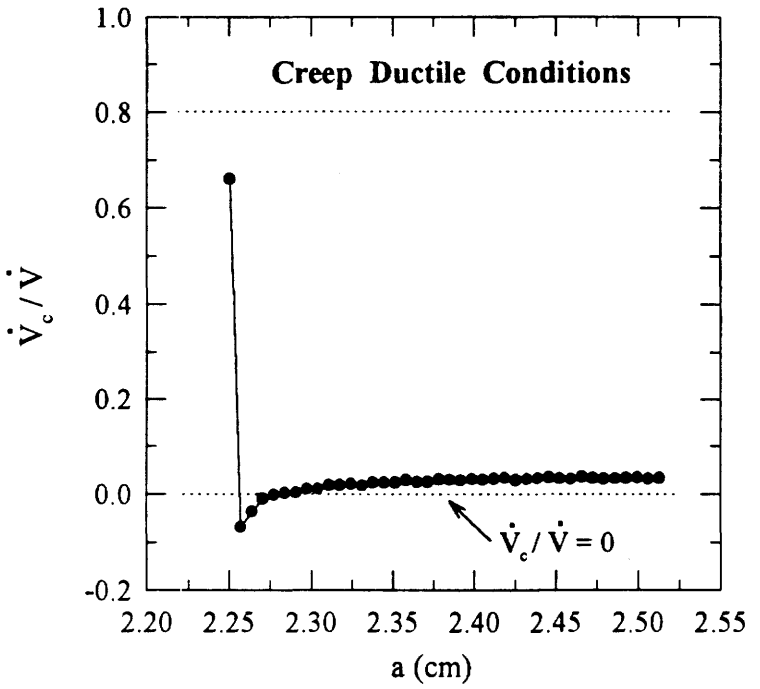

Figure 17 - Ratio of deflection rate due to creep to toal deflection rate.

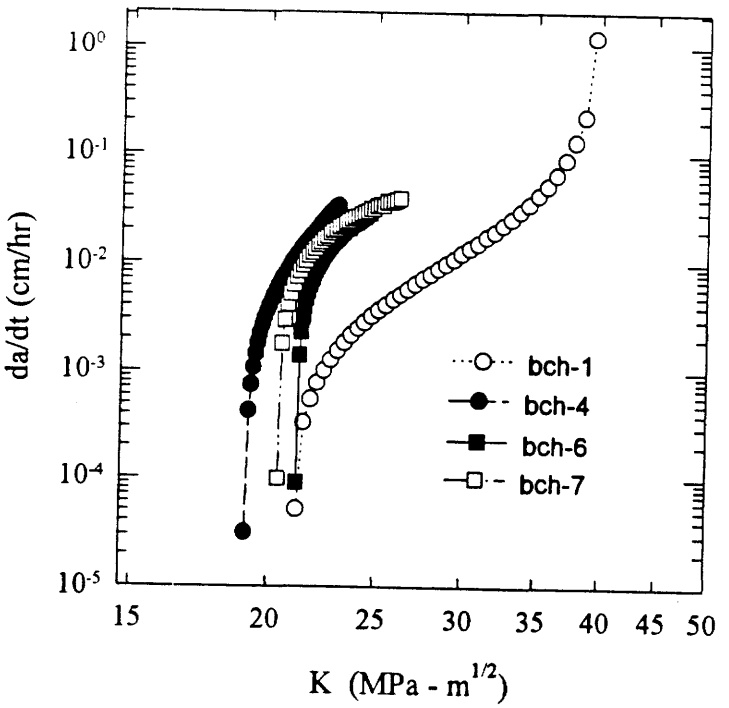

Figure 18 - Stress intensity factor versus crack growth rate.

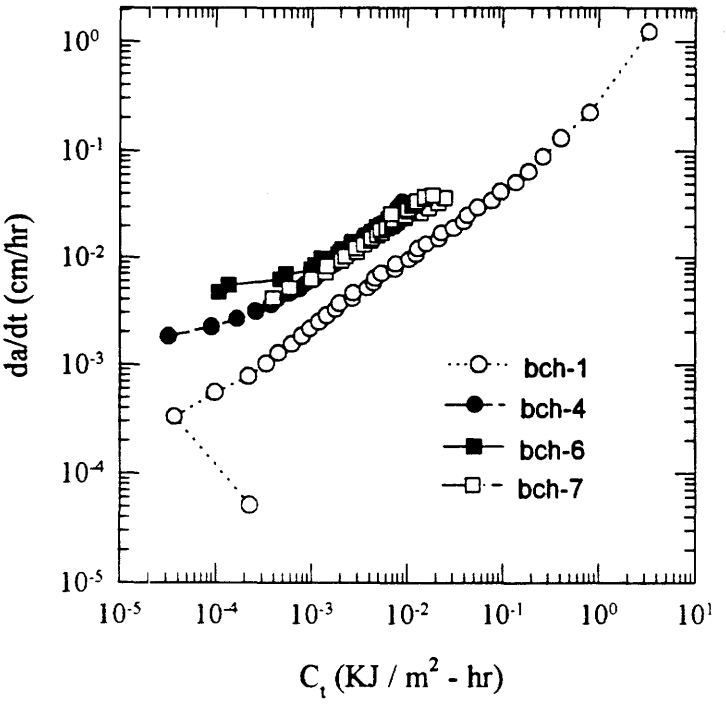

Figure 19 - The C_t parameter versus crack growth rate.

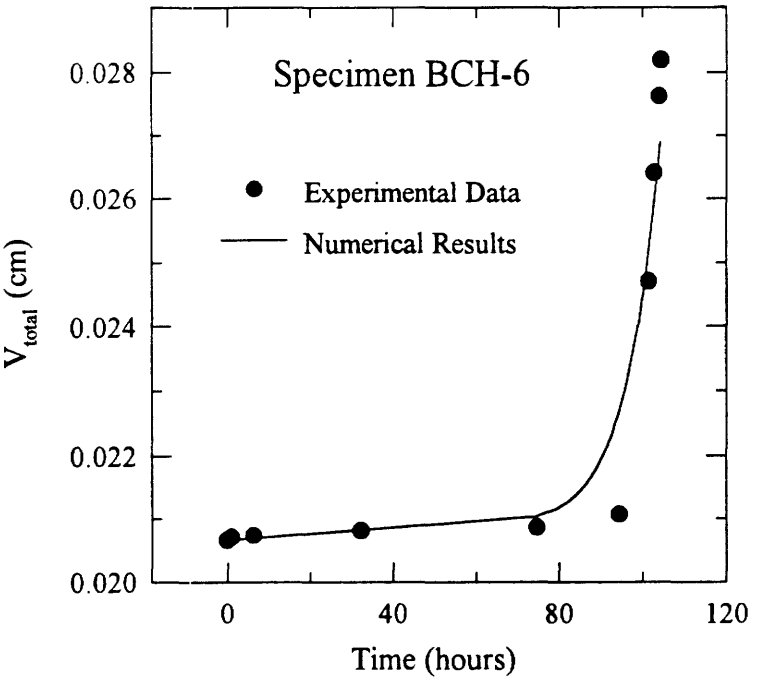

Figure 20 - Evaluation of numerical results by comparison of experimentally and numerically determined load line deflections.

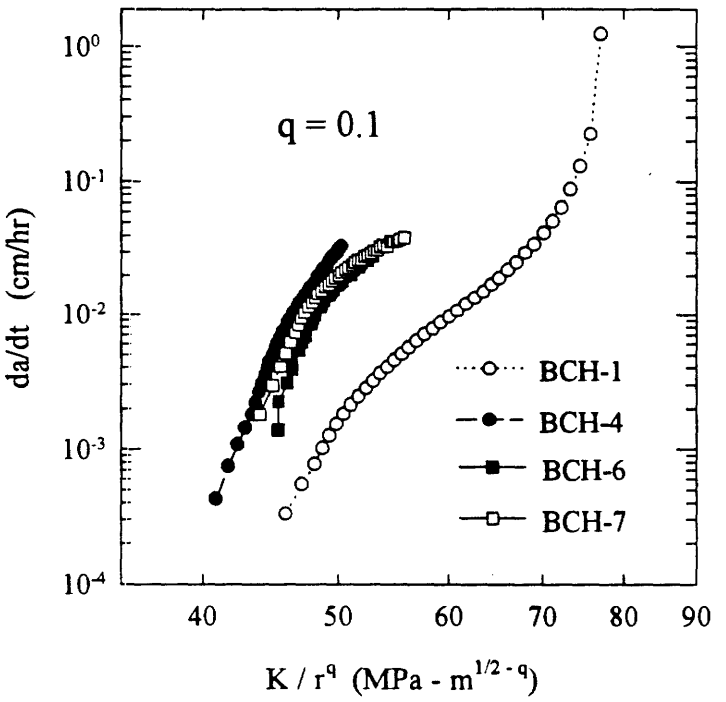

Figure 21 - K/r_c^q versus crack growth rate.

Papers presented during the

Alloys (London,

Properties of a

P 590 American

185-201

31

GA (1993)

Metals" ASTM

M E813-89

luminum Alloy:
2167-2179

tures **10** (1992)

CREEP CRACK GROWTH IN RAPIDLY SOLIDIFIED ALUMINUM ALLOY 8009

A. Saxena and K. A. Jones
School of Materials Science and Engineering
Mechanical Properties Research Laboratory
Georgia Institute of Technology
Atlanta, GA 30332-0245, USA

Abstract

Creep deformation and creep crack growth tests were conducted on a rapidly solidified aluminum alloy 8009 to evaluate the suitability of crack tip parameters such as the stress intensity parameter, K and the C_t-parameter for characterizing creep crack growth behavior. It is shown that at 316°C, the initial creep crack growth is characterized by C_t and it is characterized by K in the later portions of the test. The switch in the crack tip parameter for characterizing creep crack growth is accompanied by the establishment of a steady-state damage zone ahead of the crack tip consisting of creep cavities which nucleate at the dispersoids introduced in this material for strengthening.

Introduction

Rapidly solidified dispersion strengthened aluminum alloys (RSAA) are thermally stable at temperatures in excess of 300°C and are therefore candidate materials for high temperature structural applications[1,2] in which the creep and the creep crack growth behavior is of considerable interest.

Fracture mechanics based test methods and life prediction methodology are well developed for creep-ductile materials (creep ductility in excess of 10%)[3]. In these materials, creep crack growth is accompanied by significant creep deformation and the crack tip parameters which characterize the rates of crack growth are well established[3]. In creep-brittle materials (creep ductility on the order of 1-2 percent or less), the crack tip stress is significantly influenced by the growing crack and parameters based on the assumption that the crack tip is stationary are no longer meaningful. This limitation opens the question whether C_t or C^* can be used to characterize creep crack growth in such materials. The purpose of the research reported in this paper was to explore the limits of C_t/C^* and the stress intensity parameter, K, for characterizing the creep crack growth in 8009 Al alloy and to study the mechanisms of creep deformation and crack growth in these materials.

Materials and Specimens

The 8009 Al alloy (also known as FVS0812) has a chemical composition consisting of 8.5% Fe, 2.3% V and 1.7% Si Alloys of this composition are first rapidly solidified (cooling rates in excess of 10^5K/sec) by a planar flow casting method[4] to produce thin strips, 25μ thick. These strips are then pulverized into a powder, degassed and vacuum hot pressed into billets with about 95% density. The billet is then extruded into the final shape. In this case, the extruded thickness was 43mm of which the top and bottom 6.25mm were machined to provide a strip that was 30.5mm thick. The resulting microstructure consists of ultrafine grain size (1μ diameter) from the rapid solidification and an even distribution of dispersoids ranging in size from 30 to 80nm[4]. The dispersoids are a cubic quaternary intermetallic, $Al_{12}(Fe,V)_3Si$ which resists coarsening at temperatures less than 400°C. Therefore, the microstructure is very stable up to those temperatures.

Standard compact type specimens which were 25.4mm wide were machined in the L-T orientation and several cylindrical tensile and creep specimens were machined in the longitudinal orientation. These specimens were 2mm in diameter and 10mm in gage length. The tensile tests were performed in accordance with the ASTM standard E8-90[5], the creep deformation tests in accordance with ASTM Standard E139-83[6] and the creep crack growth tests in accordance with ASTM standard E1457-92[7]. All mechanical testing was conducted at 316°C.

The fracture surfaces of the tested compact type and creep rupture specimens were analyzed to characterize the creep cavity growth and coalescence phenomena.

Results and Discussion

The 0.2% yield strength of the test material at 25 and 316°C was 295 and 180 MPa, respectively and the ultimate tensile strength was 27.3 and 195 MPa, respectively at those same temperatures. The percent elongation to fracture was approximately 12 to 13 percent at both temperatures.

Creep Deformation and Rupture

The creep deformation behavior at 316°C and stress levels of 85.5, 100.6 and 107.0 MPa is shown in Fig. 1. The 85.4 MPa test was terminated after a steady-state creep rate was established while the other two tests were continued till rupture. The creep ductility was less than 2% in the ruptured specimens which characterizes the material as being creep-brittle. There is also significant primary creep strain present in all creep tests. Figure 1 also shows creep test results from a specimen taken from a different lot (lot II) of Al 8009 which was produced with a different thermal-mechanical treatment. The creep behavior of this specimen was quite different in comparison to those from Lot I. The Lot II was significantly more creep resistant. This lot to lot variability is a concern in comparing our results from the earlier creep crack growth data reported by Leng, et. al.[8]. It appears that the material used in the latter study was from Lot II while all our creep crack growth tests were performed on the material from Lot I.

[redacted]

isting of 8.5% Fe,
i (cooling rates in
25μ thick. These
billets with about
ase, the extruded
rovide a strip that
ize (1μ diameter)
n size from 30 to
Si which resists
very stable up to

ined in the L-T
n the longitudinal
The tensile tests
ormation tests in
accordance with

were analyzed to

and 180 MPa.
ly at those same
percent at both

d 107.0 MPa is
creep rate was
uctility was less
p-brittle. There
hows creep test
s produced with
men was quite
creep resistant.
ier creep crack
atter study was
rial from Lot I.

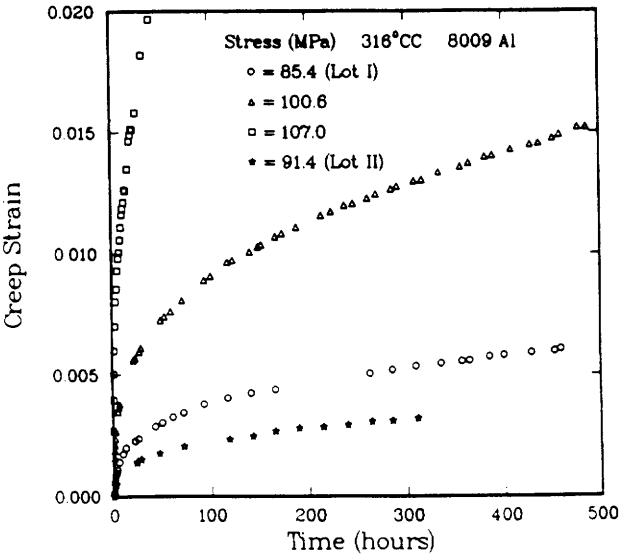

Fig. 1 - Creep Strain as a function of time at various stress levels

Fig. 2 - Creep cavities on the fracture surface of a creep rupture specimen tested at a stress of 101.6 MPa

Another observation from the creep data is the extreme sensitivity of creep rates to small variations in stress. The stress exponents for describing the secondary creep rates were on the order of 50 to 60. A possible explanation is as follows.

Alloy 8009 is a dispersion strengthened material with an aluminum matrix. When the specimen is loaded at elevated temperature, the creep rates in the Al matrix are expected to be much higher than in the dispersoids. Therefore, decohesion between the Al matrix and the dispersoids will occur resulting in the matrix carrying a higher fraction of the applied stress. Thus, a relatively small increase in nominal stress on the specimen translates into a larger increase in stress on the Al matrix because of the high volume fraction of the dispersoids. Thus, the dependence of strain rate on stress is expected to be high. Figure 2 shows a SEM fractograph from the creep specimen tested at 101.6 MPa showing the creep cavities supporting the above argument. The final cavity sizes decreased with increasing stress and also cavities did not nucleate and grow on each dispersoid. This is expected to be a stochastic process because formation of a cavity is expected to redistribute the stress and suppress the formation of other cavities in its vicinity. Also, a higher stress will tend to nucleate more cavities thus the final cavity sizes are expected to be small because rupture occurs when neighboring cavities grow and coalesce.

Creep Crack Growth

Creep cracks in alloy 8009 grow by nucleation, growth and coalescence of creep cavities as seen in Fig. 3. This figure shows the crack tip region of an interrupted creep crack growth specimen. Figure 4 shows a typical fractograph from a creep crack growth specimen showing cavitation features similar to those of the creep rupture specimen confirming that the crack growth mechanism is by creep. Figure 5 shows a plot of the cavity diameter as a function of creep crack extension for several specimens. The trend in each case was an initially increasing cavity size which reaches a maximum value and subsequently decreasing size with further crack extension.

Figures 6 and 7 show that the creep crack growth rates as a function of the stress intensity parameter, K, and the C_t parameter, respectively. Both figures also include data from two specimens tested at 150°C. This alloy exhibits a ductility minima at 150°C[8], therefore, these tests were conducted to briefly examine this phenomenon. It was observed that the rupture times of CT specimens were much shorter at 150°C compared to 316°C for tests initiated at the same K levels as expected if ductility decreases at 150°C. In this paper, we will focus primarily on the results from the 316°C tests with temperature effects being will be the subject of a future paper.

The da/dt versus K behavior shows little correlation. All tests show decreasing crack growth rates initially followed by increasing crack growth rates. The minima in crack growth rate coincides with the crack extension at which the creep cavities attain a maximum value. These results point to a relaxing stress field due to creep deformation being present during the initial portion of the tests. A decreasing crack growth rate and an increasing cavity sizes are both consistent with this conclusion. It then follows that during the initial period, the crack growth rate should correlate with C_t. This trend is in fact observed in Fig. 6 where the initial portions of the test are in the high crack growth rate region. During the later portion of the tests, no

eep rates to small
ɔ rates were on the

When the specimen
pected to be much
and the dispersoids
:d stress. Thus, a
ı larger increase in
:rsoids. Thus, the
a SEM fractograph
pporting the above
so cavities did not
ic process because
formation of other
vities thus the final
g cavities grow and

eep cavities as seen
ĸ growth specimen.
showing cavitation
the crack growth
a function of creep
ly increasing cavity
with further crack

the stress intensity
ude data from two
C^8, therefore, these
:at the rupture times
nitiated at the same
focus primarily on
subject of a future

asing crack growth
crack growth rate
mum value. These
nt during the initial
ıvity sizes are both
d, the crack growth
the initial portions
ion of the tests, no

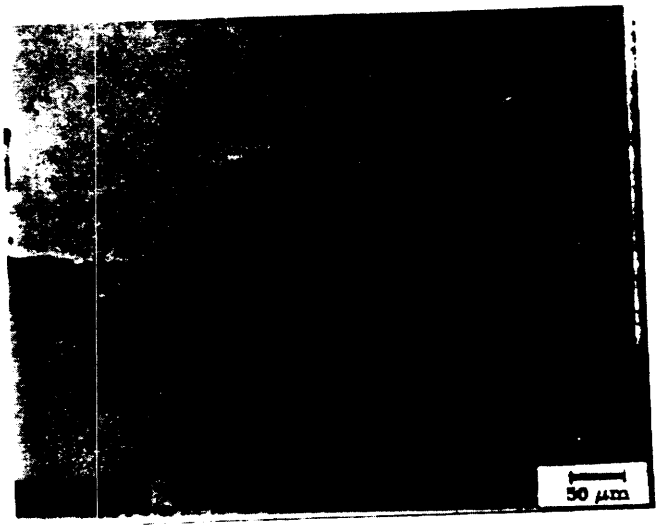

Fig. 3 - Creep cavitation damage in front of a growing creep crack

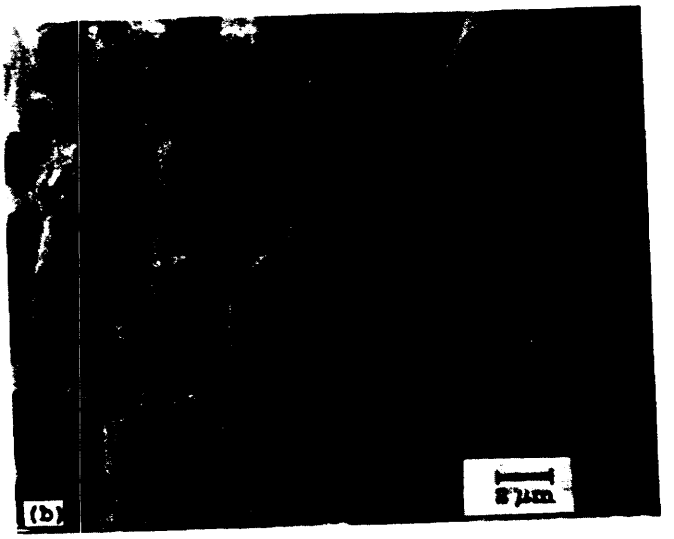

Fig. 4 - Creep cavitation on the fracture surface of a creep crack growth specimen

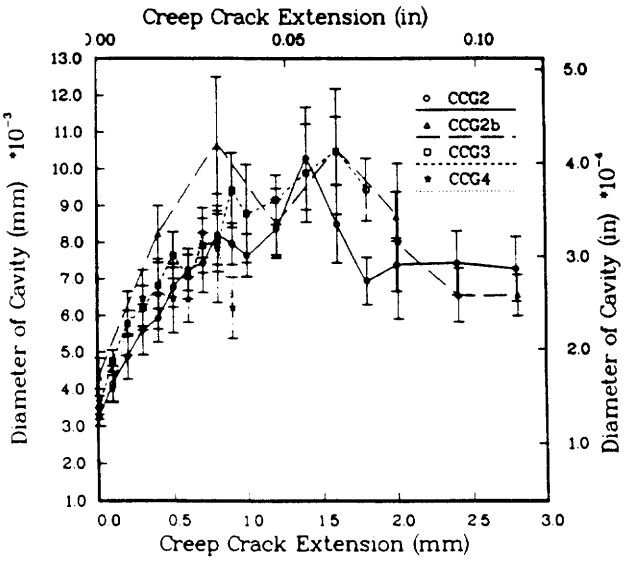

Fig. 5 - Creep cavity diameter as a function of crack extension for various creep crack growth specimens

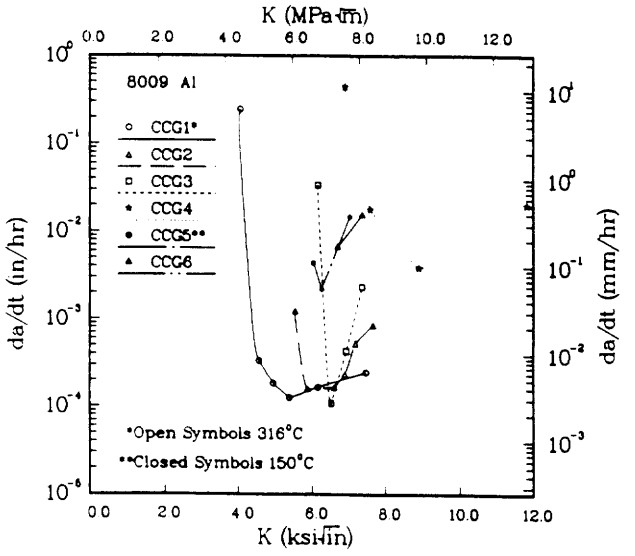

Fig. 6 - Creep crack growth rate (da/dt) versus the stress intensity parameter, K

correlation is observed between da/dt and C_t. However, plotting the data from the later portion of the test (after attainment of minima is da/dt values) shows good correlation between da/dt and K, Fig. 8. We can then conclude that after an initial period of transient crack tip stresses due to a growing creep zone size, a steady-state condition is reached during which the da/dt correlates with K. Thus, both K and C_t are relevant crack tip parameters for characterizing the creep crack growth behavior in Al alloy 8009 at 316°C. Further tests are recommended to study this trend in more depth.

p cavity
function
ision for
> crack
nens

Summary and Conclusions

1. Creep deformation rates in Al alloy 8009 at 316°C are highly sensitive to increases in stress.

2. Creep crack growth in alloy 8009 occurs by growth and coalescence of creep cavities which nucleate at the dispersoids.

3. The creep crack growth rates during the first 1.5mm of crack extension appear to correlate better with C_t and the subsequent crack extension with K at 316°C.

4. The transient period of crack extension characterized by C_t is also characterized by a rapidly changing creep cavity diameter. The cavity diameter changes much less significantly when steady-state conditions are reached and the creep crack growth rates are characterized by K.

Acknowledgements

Dr. R. Piascik of NASA-Langley Research Center supplied the test specimens. The financial support for the project was provided by the National Science Foundation Research Grant MSS-9202932. Mr. Richard C. Brown provided invaluable assistance with the experimental set up.

ep crack
(da/dt)
stress
meter, K

References

1. P.S. Gilman, et. al., "High Temperature Aluminum Alloys: Applications", Allied Signal, Inc., Corporate Technology, Morristown, NJ.

2. J.E. Benci and W.E. Frazier, Dispersion Strengthened Aluminum Alloys, ed. Y.M. Kim and W.M. Griffith, TMS, 1988, p. 131.

3. A. Saxena, Engineering Fracture Mechanics, vol. 40, No. 415, 1991, p. 721.

4. S.K. Das, The International Journal of Powder Metallurgy, vol. 24, 1988, p. 175.

5. E8-90 "Test Method for Tension Testing of Metallic Materials", ASTM Book of Standards, vol. 3-01, 1991, p. 130.

6. E139-83, "Practice for Conduction of Creep, Creep Rupture and Stress Rupture Tests for Metallic Materials," ASTM Book of Standards, vol. 3-01, 1991, p. 309.

7. E1457-92, "Standard Test Method for Measurement of Creep Crack Growth Rates in Metals", ASTM Book of Standards, vol. 03.01, 1992, p. 1031.

8. Y. Leng, W.C. Porr and R.P. Gangloff, Scripta Metallurgica, vol. 24, 1990, p. 2163.

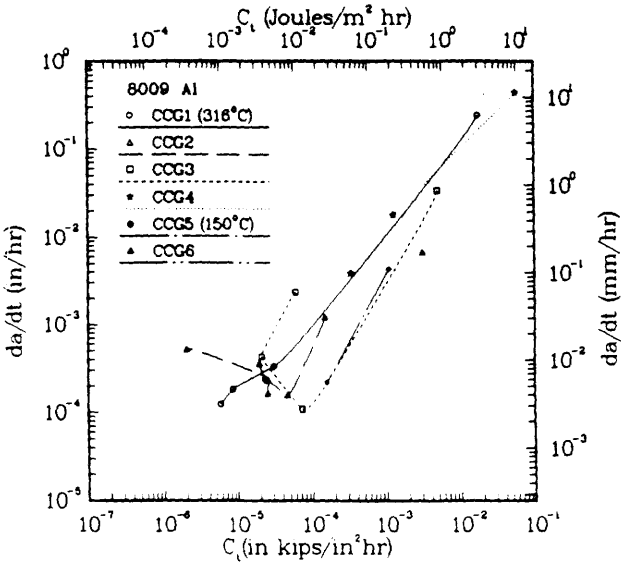

Fig. 7 - Creep crack growth rate as a function of the C_t parameter

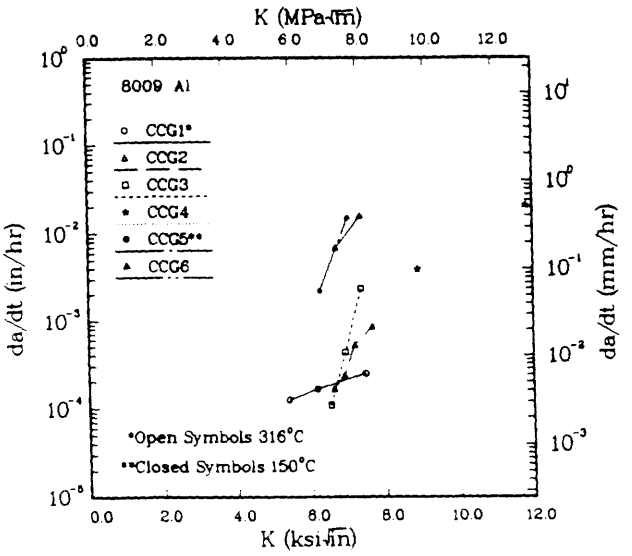

Fig. 8 - Creep crack growth rate from the portion of the test beyond minimum da/dt as a function of K

DEVELOPMENTS IN CREEP-FATIGUE CRACK GROWTH TESTING AND DATA ANALYSIS

Parmeet S. Grover[*] and Ashok Saxena[*]

Time-dependent creep-fatigue crack growth (CFCG) is a major design consideration and a factor in the estimation of remaining life for elevated temperature components. In-situ measurement of incremental changes in the load-line deflection during hold times is a key measurement in characterizing CFCG behavior. Such measurements during hold times of < 100 seconds were successfully accomplished in compact specimens for the first time. Trapezoidal waveforms with hold times of 10, 20, 50 seconds were used on 2.25Cr-1.0Mo steel specimens tested at 594°C(1100°F). A procedure for choosing a set of optimum conditions for generating CFCG data is proposed and a method for analysis is outlined.

INTRODUCTION

Improving the efficiency or achieving a longer life of new or existing energy conversion machinery is desirable. In the case of equipment such as steam headers, steam turbines, gas turbines, aircraft engines and nuclear reactors, this translates into an increase in their operating temperatures. Consideration of crack growth under creep-fatigue conditions can be the dominant factor in determining the allowable maximum stress and temperature, as well as the design and remaining lives of elevated temperature components [1]. The operation of these equipment involve start up, shutdown steps with continuous high temperature operation under sustained load being the intermediate step. Therefore, both creep and fatigue type processes influence the growth of cracks in the material. This loading history is most conveniently simulated in the laboratory by a trapezoidal loading waveshape applied to test specimens. Creep deformation occurs mainly during the sustained loading periods but it can also occur during the loading part of the cycle because the loading that occurs at high temperatures is often slow.

[*] Graduate Research Assistant and Prof. & Director, respectively, School of Materials Science and Engineering, Georgia Institute of Technology, Atlanta, GA 30332-0245, USA.

To understand the effects of these loading variables on the crack growth rate, laboratory tests which can simulate these service conditions must be developed and their results modelled mathematically. Since long test times are prohibitive due to practical constraints, accelerated test methods are needed to predict service behavior with relatively short time tests. The most challenging step in developing an *accelerated test* for CFCG testing is the measurement of incremental deflection change (ΔV) during a single hold time (t_h) of the trapezoidal loading waveform. The advantages of measured deflection values over those obtained analytically are discussed in reference [2].

In this paper, an attempt has been made to establish testing conditions, including the choice of hold time and cyclic load levels during CFCG testing such that reliable deflection measurements can be made. Further, a technique for accurate measurement of deflection change during hold time is discussed. This technique is similar to the one used during J-resistance curve testing [3] for measuring crack extension by unloading compliance.

Prior studies [4-12] have shown C_t - parameter to be the most promising for characterizing experimental CCG and CFCG data. Thus, the average value of C_t, $(C_t)_{ave}$, was used to correlate the average crack growth rate during hold time, $(da/dt)_{ave}$.

EXPERIMENTAL PROCEDURE

Material and Specimens

The test material was a 2.25Cr-1.0Mo steel taken from the hot end of an ex-service header. The uniaxial version of the constitutive law chosen to represent the creep behavior of the material is given below.

$$\dot{\epsilon} = \frac{\dot{\sigma}}{E} + A_1 \epsilon^{-p} \sigma^{n_1(1+p)} + A\sigma^n \qquad (1)$$

where σ = stress and ϵ = strain. The dots denote their respective time derivatives. E is the elastic modulus. A, A_1, n, n_1 and p are regression constants. The first term on the right hand side of Equation (1) represents the elastic strain rate and the other two represent the primary and secondary creep behaviors respectively. Most of the relevant tensile and creep properties of the material were obtained from prior studies [13]. These properties are listed in Table 1.

iables on the crack growth rate, ;e conditions must be developed ;e long test times are prohibitive iods are needed to predict service)st challenging step in developing urement of incremental deflection ie trapezoidal loading waveform. :er those obtained analytically are

to establish testing conditions, l levels during CFCG testing such made. Further, a technique for ing hold time is discussed. This l-resistance curve testing [3] for iance.

eter to be the most promising for ta. Thus, the average value of C_t, :k growth rate during hold time,

)CEDURE

: taken from the hot end of an ex- nstitutive law chosen to represent)w.

$$^{p)} + A\sigma^n \qquad (1)$$

:e their respective time derivatives. ire regression constants. The first presents the elastic strain rate and dary creep behaviors respectively. ties of the material were obtained listed in Table 1.

TABLE 1 - Material properties of 2.25Cr-1.0Mo steel at 594°C (1100°F)

Tensile Properties	Elastic Modulus × 10^{*3} *Mpa (ksi)*		Yield Stress *Mpa (ksi)*	
	161.92 (23.5)		172.25 (25)	
Plasticity Constants*	D		m	
	Mpa^{-m}	ksi^{-m}		
	1.39×10^{-13}	2.12×10^{-9}	4.99	
Secondary Creep Properties	A		n	
	$Mpa^{-n}hr^{-1}$	$ksi^{-n}hr^{-1}$		
	1.94×10^{-24}	5.41×10^{-16}	10.075	
Primary Creep Properties	A_1		n_1	p
	$Mpa^{-n_1(1+p)}hr^{-1}$	$ksi^{-n_1(1+p)}hr^{-1}$		
	8.26×10^{-28}	3.78×10^{-19}	4.92	1.1

* $\varepsilon_p = D\sigma^m$, where ε_p is the plastic strain. D and m are regression constants obtained from the true stress vs. true strain curve.

The CFCG tests were carried out using CT specimens which have become the preferred geometry in majority of fracture and crack growth test methods. These specimens offer the convenience of low test loads and the ease of instrumentation for load-line deflection measurements during hold times. The latter is because a clip-gage can be conveniently placed in the machined knife edges along the load-line and the whole assembly can be placed in a high temperature chamber. The specimens used had a width of 50.8 mm (2.0 in) and a thickness of 10.2 mm (0.4 in).

Test Conditions

All tests were carried out at 594°C (1100°F). Trapezoidal waveform was used for loading. The load levels, crack ratios, cycle times and K-levels are specified in Table 2. All these tests were carried out in air. It is noted that the rise time (t_r) and decay time (t_d), corresponding to the loading and unloading part of the cycle, respectively, were much smaller than the hold time (t_h).

Prior to the CFCG tests, a high temperature fatigue test with 1 Hz cycling frequency was also carried out at 594°C (1100°F) with the same load levels as the CFCG tests. The load levels, crack ratios and the K-levels for this test are also included in Table 2.

TABLE 2 - Description of the test conditions for the FCGR and CFCG experiments

Test Type	Hold Time	Hold Load *KN (kips)* (R = 0.1)	Crack Ratio *initial*	Crack Ratio *final*	ΔK *Mpa√m(ksi√in)* *final*
FCGR	0	5.86 (1.32)	0.3	0.4210	28.430(25.869)
CFCG	10 sec	5.86 (1.32)	0.4	0.5078	23.706(21.571)
CFCG	20 sec	5.86 (1.32)	0.4	0.4567	19.602(17.836)
CFCG	50 sec	5.86 (1.32)	0.4	0.4353	18.521(16.853)

Note:

initial value of ΔK for CFCG tests = 16.799 (15.286) *Mpa√m(ksi√in)*
initial value of ΔK for FCGR test = 12.973 (11.804) *Mpa√m(ksi√in)*

Test Equipment and Procedure

All the CFCG tests were carried out on servohydraulic machines. A high temperature stainless steel chamber was used to heat the specimen. Stainless steel leads were welded to the specimens in order to measure crack length using the 'potential drop method' [14]. The specimens were then mounted on the clevises in the chamber. The crack length, a, was calculated from the output voltages using Johnson's formula in accordance with the guidelines provided in reference [14].

A high temperature capacitance clip-gage was attached to the specimen to measure the load-line deflection. The working deflection range for the majority of the tests was 2.05 mm (0.1 in). The gage calibration was carried out at room temperature and applied to the high temperature because the calibration is not dependent on temperature in the range of 25°C to 600°C.

A strip chart recorder was used as the primary output device. It had three

atigue test with 1 Hz cycling
vith the same load levels as the
K-levels for this test are also

for the FCGR and CFCG

ck io	ΔK *Mpa√m(ksi√in)*
final	*final*
0.4210	28.430(25.869)
0.5078	23.706(21.571)
0.4567	19.602(17.836)
0.4353	18.521(16.853)

16.799 (15.286) *Mpa√m(ksi√in)*
12.973 (11.804) *Mpa√m(ksi√in)*

vohydraulic machines. A high
eat the specimen. Stainless steel
measure crack length using the
e then mounted on the clevises
ılated from the output voltages
guidelines provided in reference

as attached to the specimen to
leflection range for the majority
ibration was carried out at room
e because the calibration is not
o 600°C.

ıary output device. It had three

channels which were used for monitoring the (i) voltage change due to crack growth (ii) output voltage from the *summing amplifier* of the clip-gage for charting the load-line deflection changes during the hold times and (iii) load during the hold periods.

Use of the *unloading compliance box* was the key to the successful measurement of the incremental deflection changes during the hold time. This electronic circuit was used to subtract out the deflection change signal due to the loading part of the cycle so that the signal during the hold time could be further amplified by a factor of 10. This ensured precise measurement of deflection changes even for very short hold times (~ 10, 20 seconds). The speed of the strip-chart recorder was increased from 4 cm/hr to 4 cm/min., or in the same ratio, during the times when the output was being recorded to ensure visually clear plots of the deflection change during hold periods. Ten to twenty successive cycles were recorded each time and the average deflection change for these measurements was calculated. The crack growth during the recording of data was negligible. The number of cycles recorded in each set was varied between 10 and 20 so that the optimum number could be decided on the basis of statistical accuracy and the time involved to record each set. This information forms a part of the proposed test procedure, discussed later.

Data Reduction

The load-line displacement changes during the hold times in each cycle were read from the strip chart recorder. The mathematical mean of all the measurements in a set (10 to 20 cycles) was calculated and the result was accepted as a load-line deflection change datum if the standard deviation for the set was low ($\leq 0.25 \times$ datum). A low standard deviation ensures high quality data. The median of the cycle numbers in the set was taken as the cycle count corresponding to the displacement datum. A crack length corresponding to the deflection measurement was calculated from the recorded potential drop as described before. The crack lengths and the corresponding hold time deflection values, the material properties and the specimen dimensions were input into computer programs [2] to calculate various fracture mechanics parameters (ΔK, C^*, $(C_t)_{avg}$) and crack growth rates. The final objective was to obtain plots of $(da/dt)_{avg}$ *vs.* $(C_t)_{avg}$ and da/dN *vs.* ΔK .

Evaluation of ΔK . ΔK was evaluated as follows and was used to correlate the overall fatigue crack growth rate during a cycle, (da/dN), which is defined in equation (7).

$$\Delta K = \frac{\Delta P}{B\sqrt{W}} F\left(\frac{a}{W}\right) \tag{2}$$

where ΔP is the applied load range, B is the specimen thickness and W is the specimen width. F is an empirical factor that accounts for the specimen geometry dependence of ΔK.

Evaluation of $(C_t)_{avg}$. $(C_t)_{avg}$ can be evaluated using the measured load-line deflection change rate during hold time as follows:

$$(C_t)_{avg} = \frac{\Delta P\ \Delta V_c}{BWt_h}\ \frac{F'}{F} - \left(\frac{F'}{F}\frac{1}{\eta} - 1\right) C^*(t) \tag{3}$$

ΔP is the applied load range, ΔV_c is the load-line deflection change due to creep during hold time t_h. F is the K-calibration factor, $F = (K/P)BW^{1/2}$. $F' = dF/d(a/W)$. B is the specimen thickness and W is the specimen width. η is a function of a/W, where a is the crack length, and n *and* n_1 i.e. the creep exponents in secondary and primary creep range respectively. For CT specimens η is given by equation (4) [15].

$$\eta = \frac{n}{n+1}\left(\frac{2}{1 - a/W} + 0.522\right) \tag{4}$$

$$\Delta V_c = \Delta V - \frac{Bt_h}{P}\left(\frac{da}{dt}\right)_{avg}\left[\frac{2K_{eff}^2}{E} + (m+1)J_p\right] \tag{5}$$

where m is the plasticity exponent in the Ramberg-Osgood equation and P is the applied load level. K_{eff} is the value of K corresponding to the 'effective' crack length corrected for plasticity.

It is noted that the ΔV_c value which is obtained, using equation (5), from the total load-line deflection change, ΔV, by deflection partitioning approach [16] includes both primary and secondary creep contributions to the load-line deflection change. J_p is the fully plastic part of J and is obtained from expressions listed in Kumar et al [17]. $C^*(t)$ was determined using procedures outlined in previous research works [17] and must include the contributions of secondary and primary creep.

(2)

n thickness and W is the
or the specimen geometry

g the measured load-line

$$\left.\right) C^*(t) \qquad (3)$$

ection change due to creep
$F = (K/P)BW^{1/2}$. F' =
e specimen width. η is a
n and n_t i.e. the creep
ctively. For CT specimens

$$\left.\right) \qquad (4)$$

$$(m+1)J_p\Big] \qquad (5)$$

sgood equation and P is the
ding to the 'effective' crack

using equation (5), from the
partitioning approach [16]
ns to the load-line deflection
ed from expressions listed in
edures outlined in previous
ns of secondary and primary

Determination of $(da/dt)_{avg}$. The average crack growth rate during hold time, $(da/dt)_{avg}$, was calculated as follows.

$$\left(\frac{da}{dt}\right)_{avg} = \frac{1}{t_h}\left[\left(\frac{da}{dN}\right) - \left(\frac{da}{dN}\right)_{cycle}\right] \qquad (6)$$

$(da/dN)_{cycle}$ is the cyclic crack growth rate and was obtained from the 1 Hz FCGR test carried out prior to the CFCG tests. The overall crack growth rate during a fatigue cycle, (da/dN), is defined as

$$\frac{da}{dN} = \left(\frac{da}{dN}\right)_0 + \int_0^{\frac{1}{\nu}} \left(\frac{da}{dt}\right) dt \qquad (7)$$

where $(da/dN)_0$ is the crack growth rate at a higher frequency ν. (da/dt) is the time-dependent crack growth rate.

RESULTS AND DISCUSSION

CFCG Behavior

The CFCG behavior of 2.25Cr-1.0Mo steel was characterized and a model has been proposed to estimate the crack growth rates for this material under trapezoidal loading waveshapes. ΔK and $(C_t)_{avg}$ have been used as the correlating parameters for the cycle dependent and time dependent crack growth rates respectively.

The 1 Hz frequency FCGR test data was used to calculate the cycle dependent crack growth rate, $(da/dN)_{cycle}$, and to obtain the Paris constants by regression analysis. Figure 1 is the graph of this data and the fatigue crack growth data obtained with various hold times. The linear regression line generated from this data is also shown.

The fatigue crack growth rate with various hold times plotted as a function of ΔK in Figure 1 is scattered, as expected, because ΔK is not suitable for characterizing the time-dependent crack growth rate during hold period. An increase in da/dN with increasing hold time for fixed ΔK is observed. This is due to the increasing contribution of time-dependent crack growth.

C_t was used as the correlating parameter for time dependent crack growth rate.

Figures 2 is the graph of *da/dt* vs. C_t for the CCG data [18] and $(da/dt)_{avg}$ vs. $(C_t)_{avg}$ for the CFCG data. The loading and unloading parts of the trapezoidal waveform used in the CFCG tests were the same as those for the triangular waveform employed in the FCGR test while the hold times varied from 10 seconds to 50 seconds. Crack growth behavior was considered completely cycle dependent for the loading and unloading portions of the trapezoidal waveform while the crack growth during the hold time was considered as being only time dependent. The *measured* $(C_t)_{avg}$ values are plotted against $(da/dt)_{avg}$ in Figure 2. An excellent correlation between all CCG and CFCG data is observed and all data fall on a single trend when *da/dt* is characterized in terms of C_t and $(da/dt)_{avg}$ in terms of $(C_t)_{avg}$. This has the important implication that life prediction procedures for this material would be considerably simplified because CCG data could be used to predict the life of components under CFCG conditions and vice-versa. The time dependence of the model was obtained by generating a regression line through the data in Figure 2.

Combining the cycle and time dependent crack growth rates, we express below the model for total fatigue crack growth rate per cycle under trapezoidal waveshapes.

$$\frac{da}{dN} = 1.08\times10^{-6}\ \Delta K^{1.94} + 1.46\times10^{-2}\ \left[(C_t)_{avg}\right]^{0.722}\ t_h \qquad (8)$$

The above equation can be effectively used to predict the service life of high temperature components made of 2.25Cr-1.0Mo steel under, both, CCG and CFCG conditions at 594°C (1100°F). This model has been established under the assumption that the crack growth during hold time is only due to creep deformation. Any other time-dependent effects like oxidation at the crack tip have not been incorporated. Neither have any synergistic effects due to any complicated interactions of the creep and fatigue mechanisms of crack growth during unloading/reloading been incorporated. Despite these simplifying assumptions, the CCG and CFCG data at various hold times collapses into a single trend.

Recommended Method for CFCG Testing

Outline of the Steps in Conducting a CFCG Test .

(1) Material properties needed:
- (i) Elastic properties - Young's Modulus (E)
- (ii) Yield strength (σ_{ys}^{c})
- (iii) Plastic properties - D, m
- (iv) Primary creep properties - A_1, n_1, p
- (v) Secondary creep properties - A, n

3] and $(da/dt)_{avg}$ vs.
s of the trapezoidal
e for the triangular
ies varied from 10
ed completely cycle
apezoidal waveform
l as being only time
$da/dt)_{avg}$ in Figure 2.
observed and all data
f C_t and $(da/dt)_{avg}$ in
prediction procedures
CCG data could be
tions and vice-versa.
ting a regression line

th rates, we express
cle under trapezoidal

$$\left.\right]^{0.722} t_h \qquad (8)$$
g]

he service life of high
both, CCG and CFCG
established under the
s only due to creep
on at the crack tip have
due to any complicated
crack growth during
ifying assumptions, the
a single trend.

(E)

The creep properties are the regression constants in the constitutive creep law that the material obeys (equation 1 in this study). It is important to note that fairly accurate estimates of $(C_t)_{avg}$ can be made using Equation 3 even when accurate values of creep constants are not available because for CT specimens $(F'/F)/\eta \approx 1$.

(2) Selecting the specimen geometry and size:

The following factors should be considered in selecting the specimen size and geometry:-

(i) CT specimens have an advantage over CCT specimens because the transition time for extensive creep conditions to develop is longer for the same K and a/W. Due to the longer transition times in the CT specimens, the condition that $t_c/t_t \ll 1$ is more easily satisfied and ΔK is a meaningful characterizing parameter for longer hold times and crack sizes, provided the time independent plasticity is negligible and small scale yielding (SSY) conditions prevail [19]. t_c is the cycle time and t_t is the transition cycle time defined for extensive creep conditions to develop. Another advantage of the CT specimen is that a clip-gage to measure deflection can be placed conveniently at the load-line.

(ii) Constraints pertaining to the amount of material available can also be instrumental in deciding the specimen dimensions especially if the orientation of the specimen is dependent on the location of cracks in the material.

(iii)The size/shape of the furnaces and load capacity of the test machines can also affect the choice of specimen size.

(3) Selecting the waveshape for loading:

The loading waveshape should simulate the actual loading conditions. For power-plant components, this is very often a trapezoidal waveform. The rise/decay and hold times should be decided for a trapezoidal waveshape with a hold at maximum load. Other waveforms, with hold times at minimum load or negative load ratios may be employed, if needed.

(4) Choosing the K-levels/load-levels:

This choice depends on the crack growth rates required during the test. Ideally, crack growth rates should be approximately those encountered by the material during service. However, quite often the time available for generating creep-fatigue data dictates the selection of the crack growth rates. For example, if the test data are desired within one month, an average crack-growth rate can be obtained by dividing the expected crack extension by the total number of cycles that can be applied in one month. Since the number of fatigue cycles enter into the equation, the K-levels for the test can be selected only in conjunction with the

hold time, which is discussed next.

(5) Selecting the hold times:

In addition to simulating the service conditions, other factors enter into selecting the length of the hold time as follows:-

(i)The hold time should be selected in conjunction with the K-level such that crack extensions on the order of 5 mm (0.2 inches) are obtained during the planned duration of the test. When testing a new material, trial and error is often necessary to select the appropriate K-level/hold-time conditions.

(ii) Sensitivity of the displacement-gage available for measuring the load-line deflection change is also a factor in selecting the hold time. Since this measurement is the key to a successful CFCG test, the hold time should be selected such that the deflection which accumulates during the hold time is approximately three to five times the sensitivity of the displacement-gage/amplifier system used. Again, trial tests may be necessary when testing a new material to establish that this is in fact the case.

(iii) The hold time chosen should be no more than, approximately, fifty percent of the calculated transition time for the expected final crack size in the test.

(6) Selecting the test temperature:

Test temperature should be the same as the service temperature. Higher temperatures may be used to decrease the test duration, however, caution must be exercised in selecting the test temperature. It is essential to ensure that the deformation and cracking mechanisms do not change substantially when higher temperatures are employed.

(7) Type of test to be conducted:

Either load control or displacement control tests can be conducted. However, while conducting a load control test, SSY conditions should be ensured.

(8) Required Measurements from the test:

The measurements to be made during the test are the deflection change during hold time, total load-line deflection and the crack length corresponding to different stages of the test i.e. the a vs. N data, where N = number of cycles. It is advisable to monitor the load during the hold time to ensure that the deflection changes are not due to any random variations in the load. The load-line deflection data can be obtained using a high temperature clip-gage, calibrated at room temperature and placed along the load-line of the CT specimen. In order to increase the sensitivity of the deflection change output, the deflection signal during the loading portion of the cycle should be electronically subtracted out and the

ıs, other factors enter into

)njunction with the K-level
of 5 mm (0.2 inches) are
f the test. When testing a
n necessary to select the
s.
available for measuring the
actor in selecting the hold
to a successful CFCG test.
that the deflection which
pproximately three to five
nent-gage/amplifier system
ssary when testing a new
the case.
more than, approximately,
time for the expected final

ervice temperature. Higher
n, however, caution must be
ssential to ensure that the
e substantially when higher

)l tests can be conducted.
onditions should be ensured.

st are the deflection change
rack length corresponding to
re N = number of cycles. It
to ensure that the deflection
oad. The load-line deflection
lip-gage, calibrated at room
CT specimen. In order to
it, the deflection signal during
ically subtracted out and the

signal during the hold time should be amplified. It is important to point out that this also amplifies the noise which may need to be filtered from the signal. A strip-chart recorder is very useful in recording the output deflection traces which can be visually examined to assess the quality of the data obtained. It is the authors' view that good and bad data may be easier to recognize on a strip-chart record than in one obtained from a computerized data acquisition system. Since, only a strip-chart recorder was used in this study, a fair evaluation of the efficacy of a computerized data acquisition system as an output device for this application is not possible. However, it is suggested that a strip-chart recorder be used at least as a backup device for recording the output. The crack length data must be obtained by 'non-visual techniques'. Electric potential drop method (DC and AC) have been widely used. In this study, DC potential drop was used with satisfactory results. The details of this technique were discussed earlier in [2] and are also described in Reference [20].

(9) Presentation of the Test Results:

Whenever CFCG testing is carried out for a material, it is suggested that the $(da/dt)_{avg}$ vs. $(C_t)_{avg}$ data be compared with the da/dt vs. C_t data from CCG tests on the same material because if they show the same trend, life estimation procedures for the material can be simplified, as discussed earlier.

Along with the explanation of the test conditions used, the results from the development of the test procedure should include information on the characterization of the crack growth behavior of the material. Comprehensive analytical schemes for the prediction of crack growth rates under any given set of loading conditions and hold times are preferable.

Additional Suggestions for Collecting Data . In this study all the CFCG tests were carried out as per the outline presented above. Figure 3 shows a set of good data. However, during the course of testing and analysis of the results, certain interesting observations were made which should be kept in mind while carrying out CFCG tests according to the proposed test methodology.

(1) Racheting - The clip-gage which was calibrated for an opening of 2.54 mm (0.1 inch) corresponding to 10 volts saturated earlier (fewer cycles and crack extension) during the 50 second hold time test as compared to the 20 second hold time test. Therefore, racheting is more a concern with longer hold times. It was observed that towards the end of the 10 second hold time test (ie. the end of the gage's range), the crack growth rates were very high. Thus, greater care and recording a greater number of measurements towards the end of the test is suggested.

(2) On the basis of observations made while collecting and analyzing the

data, it is proposed that corresponding to each set of deflection change measurements there should be two crack length measurements and total deflection measurements made, preferably during the first and last cycles of the set. The average of the two crack lengths should be used as the crack length for the average deflection change obtained from the set of measurements. This would account for any erratic behavior in the crack growth, which could be the case as shown in Figure 4. This is a photograph of the actual test data from the 20 second hold time test.

(3) On several occasions deflection change data had to be discarded due to high noise to signal ratio in the output. Figures 5 and 6 are examples of this situation. This noise could be due to the fluctuations in the electrical/electronic circuitry associated with the gage or the gage itself not being perfectly aligned. This was more prevalent during the 10 seconds hold time test. This was probably because during this short hold time the gage did not get sufficient time to stabilize before displacement direction got reversed due to unloading. This explains why in case of the 2.25Cr-1.0Mo steel the 50 second hold time data was the 'cleanest', virtually noise free as shown in Figure 3.

(4) It is suggested that, if possible, the same calibration be used on the strip-chart recorder throughout the test in order to minimize any errors during visual inspection of data for measuring the deflection change. However, the calibration chosen should be such that significant deflection change is visible in each cycle so that the accuracy of measurement from the strip-chart is not compromised.

CONCLUSIONS

An accelerated test procedure for creep-fatigue crack growth (CFCG) testing has been developed and the various steps in conducting tests and analyzing data are outlined and discussed. The CFCG behavior of 2.25Cr-1.0Mo steel at 594°C (1100°F) has been characterized following the proposed test procedure. A model has been presented which can be used for assessing the residual life and/or safe inspection intervals for 2.25Cr-1.0Mo steel components under trapezoidal waveshape loading at 594°C (1100°F). The following conclusions can been drawn from this study:

(1) The accelerated test procedure that has been developed shows promise for use for CFCG testing, as demonstrated by the successful testing carried out on 2.25Cr-1.0Mo steel for characterizing its behavior at 594°C (1100°F) under trapezoidal waveshape loading conditions. Detailed methods have been developed that allow one to utilize the existing extensometry on CT specimens for obtaining reliable load-line displacement changes during the hold-time. This is the keystone in the development of a successful test methodology. However, a more extensive

set of deflection change
rements and total deflection
ast cycles of the set. The
s the crack length for the
neasurements. This would
which could be the case as
tual test data from the 20

had to be discarded due to
and 6 are examples of this
s in the electrical/electronic
not being perfectly aligned.
ime test. This was probably
et sufficient time to stabilize
loading. This explains why
time data was the 'cleanest'.

bration be used on the strip-
ize any errors during visual
ge. However, the calibration
ange is visible in each cycle
chart is not compromised.

k growth (CFCG) testing has
tests and analyzing data are
.25Cr-1.0Mo steel at 594°C
sed test procedure. A model
the residual life and/or safe
mponents under trapezoidal
g conclusions can been drawn

developed shows promise for
cessful testing carried out on
r at 594°C (1100°F) under
methods have been developed
n CT specimens for obtaining
old-time. This is the keystone
. However, a more extensive

study on different materials is recommended to further develop this technique.

(2) Ideal conditions for the CFCG testing of 2.25Cr-1.0Mo steel at 594°C (1100°F) have been presented. It is suggested that a hold time of 50 seconds and a rise and decay time of 0.5 seconds represent ideal conditions for CFCG testing.

ACKNOWLEDGEMENTS

The authors would like to thank Mr. R.C.Brown for his assistance during the testing. Appreciation is also due to Mr. R. Norris for his help at various stages.

REFERENCES

[1] Saxena, A., JSME Int. J. Series A, Vol. 36, No. 1, pp 1-20.

[2] Grover, P.S., "M.S. Thesis", School of Materials Sc and Eng. , Georgia Inst. Of Technology, Atlanta, GA, U.S.A., 1993.

[3] ASTM Book of Standards, ASTM Standard 1152-87., Vol. 03.01, pp 825-835, 1991.

[4] Saxena, A., Williams R.S. and Shih, T.T., In "Fracture Mechanics: Thirteenth Conference", ASTM STP 743, pp 86-99, 1981.

[5] Swaminathan, V.P., Shih, T.T. and Saxena, A., Eng. Frac. Mechanics, Vol. 16, No. 6, pp 827-836, 1982.

[6] Saxena, A. and Gieseke, B., in "International Seminar on High Temperature Fracture Mechanics and Mechanics", EGF-6 Elseveir Publications, Vol. III, pp 19-36, 1990.

[7] Gieseke, B. and Saxena, A., "Advances in Fracture Research: Proceedings of the Seventh International Conference of Fracture-ICF 7". Edited by K. Salama et al. , Pergamon Press, pp 189-196, 1989.

[8] Saxena. A, in "Fracture Mechanics: Seventeenth Volume", ASTM STP 905, pp 185-201, 1986.

[9] Saxena, A. and Han, J. "Evaluation of Crack Tip Parameters for Characterizing Crack Growth Behavior in Creeping Materials". Technical Report , Fracture and Fatigue Research Laboratory, Georgia Inst. of Technology, ASTM Joint task Group E24.08.07/E24.04.08, 1986.

[10] Riedel, H. and Detampel, V, Int. J of Fracture, Vol 33, pp 239-262, 1987.

[11] Kuhnle, V. and Riedel, H., Int. J. of Fracture, Vol. 34, pp 179-194, 1987.

[12] Yoon, K.B., "Doctoral Thesis", School of Mechanical Eng, Georgia Inst. of Technology, Atlanta, GA, U.S.A., 1990.

[13] Saxena, A., Han, J. and Banerji, K., J. of Pressure Vessel Tech., Vol 110, pp 137-146, May 1988.

[14] ASTM Standard E1457-92, "ASTM Book of Standards", Vol. 03.01, pp 1031-1043, 1992.

[15] Liaw, P.K., Saxena, A. and Shaefer, J., in Engineering Fracture Mechanics, Vol. 32, pp 675 , 1989.

[16] Saxena, A., Ernst, H.A. and Landes, J.D., Int. J of Fracture, Vol. 23, pp 245-257, 1983.

[17] Kumar, V., German, M.D. and Shih, C.F. "An Engineering Approach to Elastic-Plastic Analysis". Technical Report EPRI NP-1931, Electric Power Research Institute, 1981.

[18] Liaw. P.K. and Saxena, A., Unpublished Data, Westinghouse Science and Technology Center, Pittsburgh, PA 15235, U.S.A., 1990.

[19] Saxena, A., "Basic Questions in Fatigue: Volume II", ASTM STP 924, pp 27-40, 1988.

[20] ASTM Standard E647-91, ASTM Book of Standards, Vol 03.01, pp 654-681, 1991.

Vol 33, pp 239-262, 1987.

Vol. 34, pp 179-194, 1987.

:hanical Eng, Georgia Inst.

ure Vessel Tech., Vol 110,

Standards", Vol. 03.01, pp

neering Fracture Mechanics,

. J of Fracture, Vol. 23, pp

n Engineering Approach to
RI NP-1931, Electric Power

., Westinghouse Science and
S.A., 1990.

ime II", ASTM STP 924, pp

andards, Vol 03.01, pp 654-

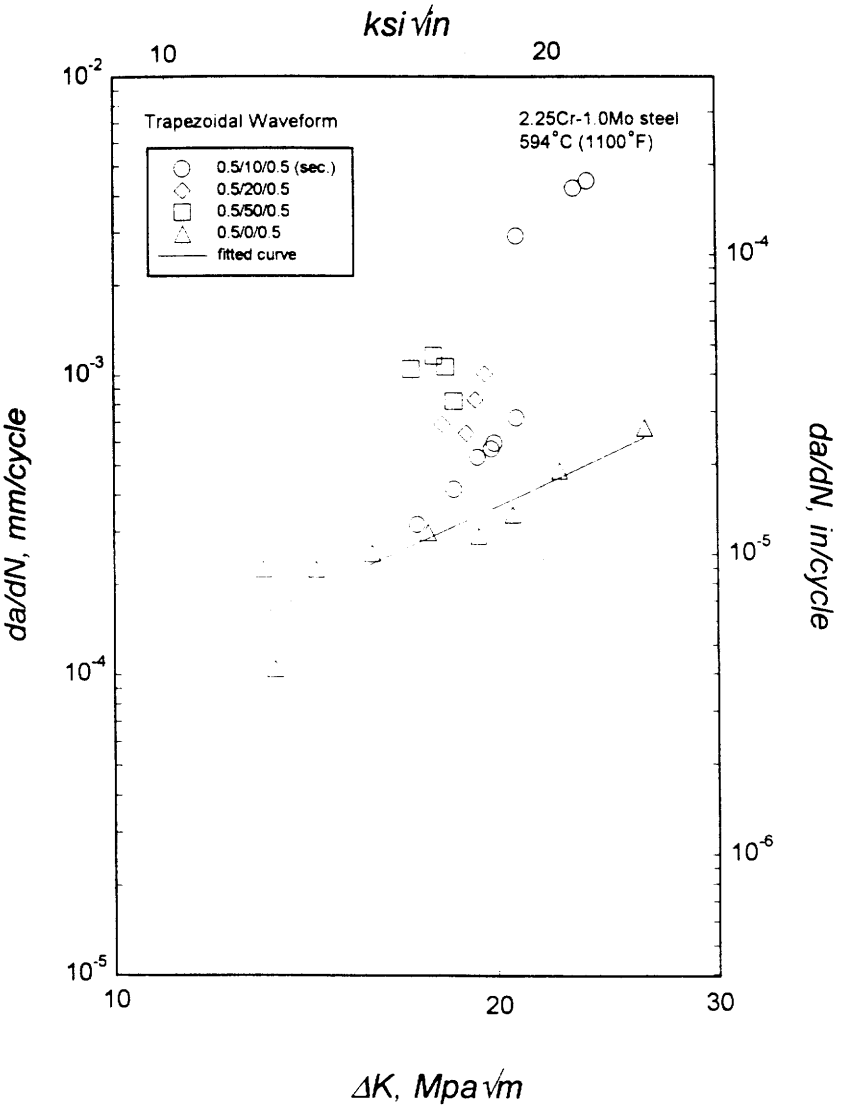

Figure 1 Fatigue crack growth data with various hold times and without hold time.

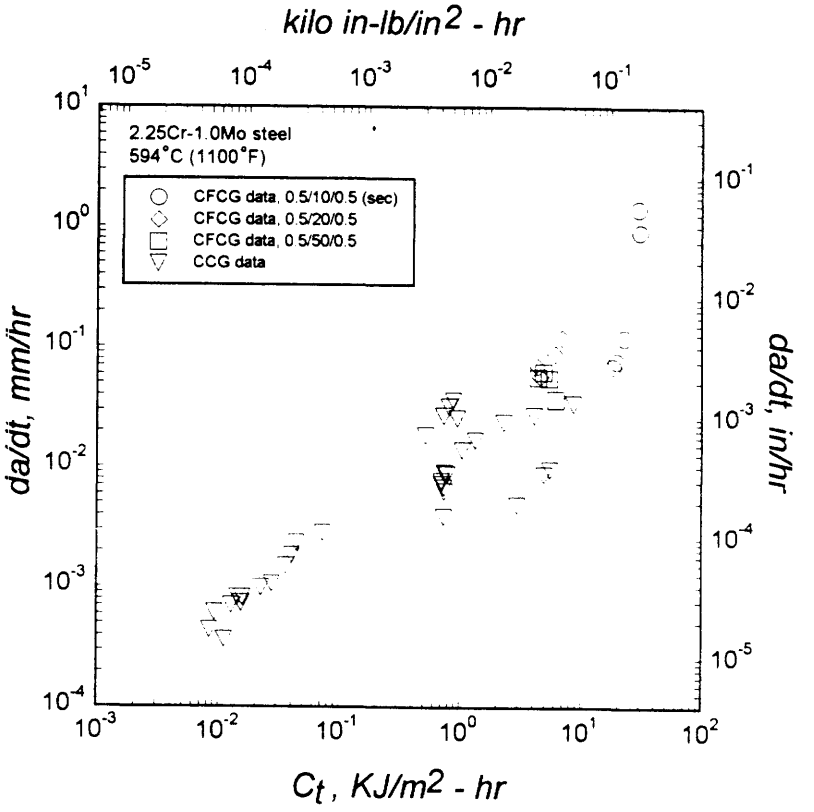

Figure 2 Correlation of the crack growth rates with the measured values of C_t. (The average values of *da/dt* and C_t are plotted for CFCG data)

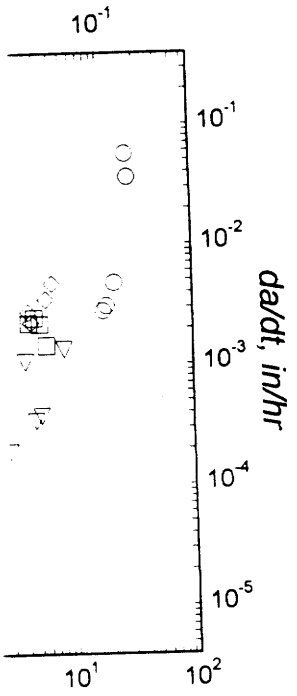

es with the measured values of
ıd C_t are plotted for CFCG data)

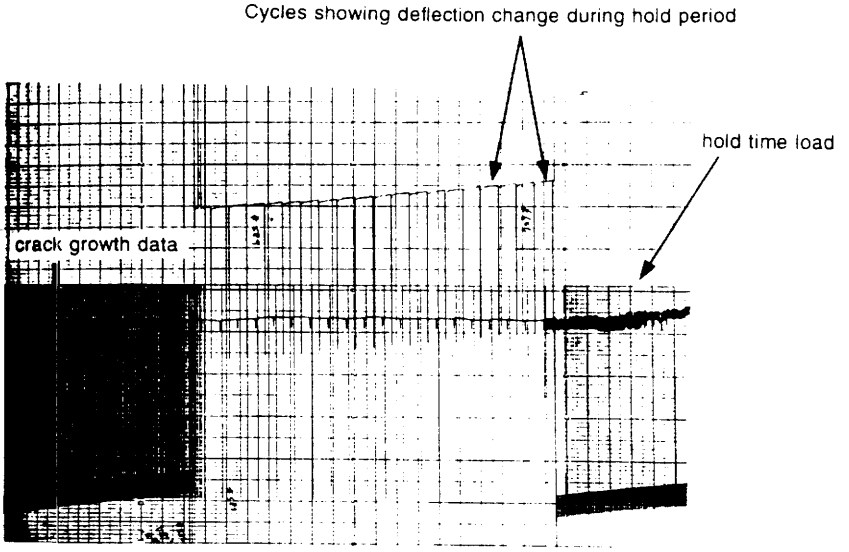

Figure 3 Good deflection change data from the strip chart.

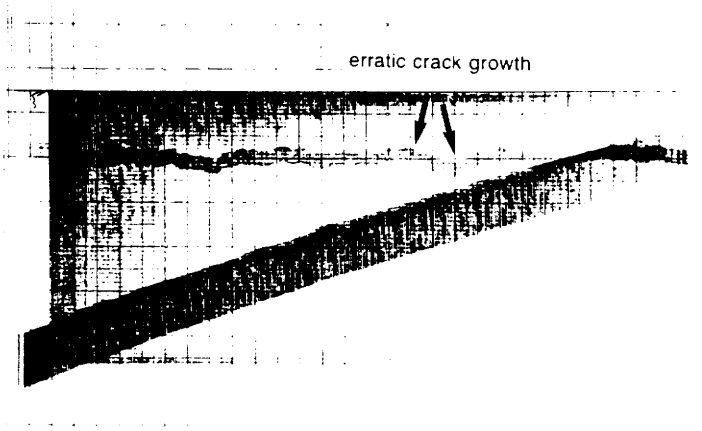

Figure 4 Erratic behavior in crack growth (from the 20 seconds hold time data)

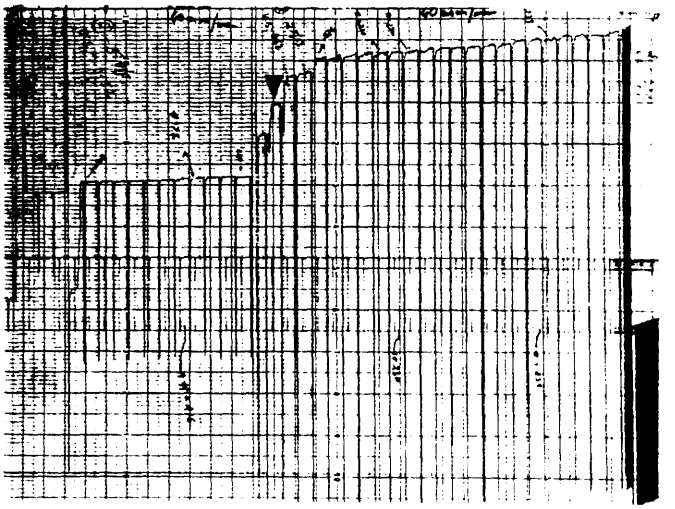

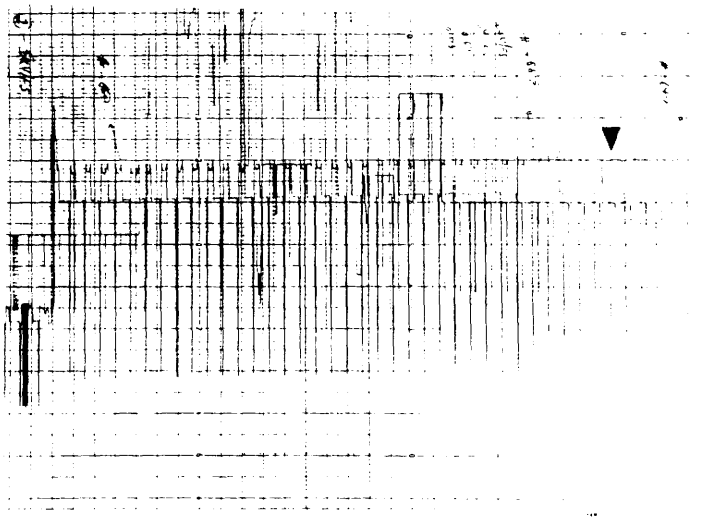

Figure 5 Examples of noise in the data (10 seconds hold time test).

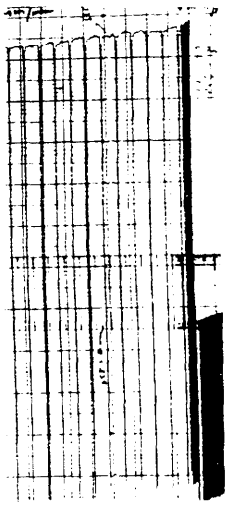

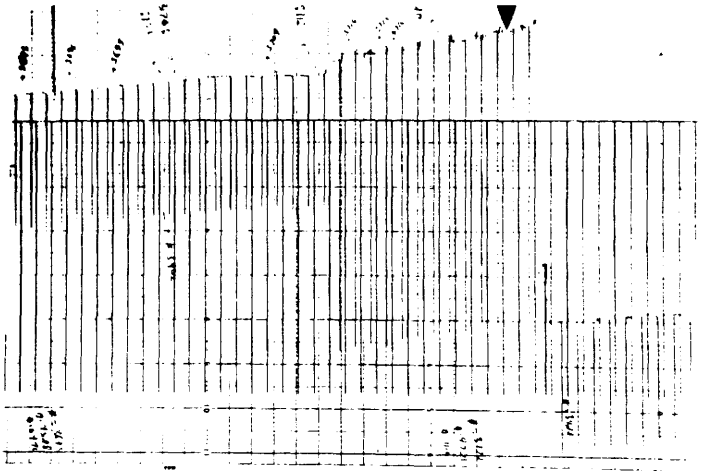

Figure 6 Another example of noise in the data (20 seconds hold time data).

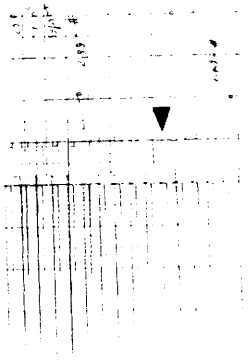

10 seconds hold time test).

Some Aspects of Crack Growth in Creep-Brittle Materials

David E. Hall, David L. McDowell, and Ashok Saxena

Georgia Institute of Technology, Atlanta, Georgia, U.S.A.

1. INTRODUCTION

Much research to date has focused on creep-ductile materials where crack growth is accompanied by significant accumulation of creep deformation in the cracked body. Less attention has been devoted to creep-brittle materials which exhibit more rapid crack growth rates in the presence of limited creep deformation. Creep-ductile and creep-brittle materials have significantly different creep zone shapes during crack growth. Moreover, the mechanisms for crack growth may differ.

During crack growth, the rate of deflection at the load-line is dependent on the rate of accumulation of creep deformation in the cracked body. Saxena and Landes [1] showed that the total load-line deflection rate ($\dot{V}$) could be decomposed into an elastic component ($\dot{V}_e$), a plastic component ($\dot{V}_p$) and a creep component ($\dot{V}_c$). For creep-ductile crack extension where the load line deflection rate is dominated by creep deformation according to $\dot{V}_c/\dot{V} > 0.8$, they found that the time-dependent fracture parameter C_t [2] appropriately correlated with the crack growth rate. When the deflection at the load line is not dominated by creep deformation, the $\dot{V}_c/\dot{V}$ ratio decreases and may even become negative so that $\dot{V} \approx \dot{V}_e$. Recent research shows that correlation of the crack growth rate with K and small (or negative) values of $\dot{V}_c/\dot{V}$ are typical characteristics of creep-brittle materials [3]. Some fundamental differences in creep-brittle and creep-ductile crack growth are highlighted in this paper.

2. SIMULATION OF CREEP-BRITTLE & CREEP-DUCTILE CRACK GROWTH

2.1 Numerical model

Finite element analyses are carried out using a small strain code developed by Leung and McDowell [4] based on an implicit trapezoidal time stepping scheme.

Crack growth is simulated by releasing a sequence of finite element nodes along the crack growth path at a specified rate using an algorithm similar to those of Hawk and Bassani [5] and Moyer and Liebowitz [6]. As the crack grows from one nodal position to the next, the net force on the node to be released is gradually relaxed over a number of time steps. Instead of releasing the node over a prescribed number of force decrements, an opening displacement is imposed on the node to be released to ensure that the rate of force release due to crack growth is faster than the rate of force relaxation due to creep. Application of these displacement increments ensures that the crack immediately begins to open. Increments of displacement are continued (based on

the previously released nodes overall y-direction displacement) until the net force on the node is reduced to a fraction of its original value or until a specified time is reached. The remaining force on the node is then reduced to zero by applying force decrements over a number of time steps.

The new variable time step, nodal release approach devised here selects a new time step for each displacement increment or load decrement according to the most conservative of three time stepping criteria. First, the effective creep strain expected to be accumulated at any gauss point during the current time step should be less than or equal to some fraction (τ) of the total effective strain at that gauss point, so that

$$\Delta t_{max} \leq \tau \left(\frac{\bar{\varepsilon}}{\dot{\bar{\varepsilon}}_c} \right), \tag{1}$$

where $\bar{\epsilon}$ is the total effective strain and $\dot{\bar{\epsilon}}_c$ is the effective creep strain rate. Another useful limit can be imposed to avoid oscillatory solutions which often occur if the time step changes too abruptly,

$$\Delta t_{max} \leq k \, \Delta t_{old} , \tag{2}$$

where k is a specified constant and Δt_{old} is the previous time step length. The third limit on the time step requires that a minimum number of time steps be completed during the release of a node according to

$$\Delta t_{max} \leq \frac{t_{end} - t_{start}}{N + M} , \tag{3}$$

where N and M are guesses for the number of displacement increments and load decrements, respectively, and t_{start} and t_{end} are the times at which release of the current crack tip node begins and ends, respectively.

After choosing the minimum of the Δt_{max} values in (1)-(3) above, the displacement increment or load decrement is computed based on this time step. Displacements are prescribed until the remaining reaction at the crack tip node is less than ten percent of the initial reaction ***OR*** until a specified amount of time (t_{switch}) has elapsed:

$$t_{switch} = (t_{end} - t_{start}) \left(\frac{N}{N + M} \right) . \tag{4}$$

Here, t_{switch} is the maximum period of time during which displacements are incremented. Displacement increments are given as

$$\Delta V = V_{ref} \left(\frac{\Delta t}{t_{switch}} \right) , \tag{5}$$

where V_{ref} is the y-displacement at the node behind the crack tip at $t=t_{start}$. When the reaction at the node has been reduced to ten percent of its initial value or the y-displacement at the crack tip node is equal to V_{ref}, the remaining load on the node is reduced to zero over two or more time steps. The load decrements at the crack tip, denoted as ΔR_y, are given by

$$\Delta R_y = -R_y \left(\frac{\Delta t}{t_{end} - t + \Delta t} \right) , \tag{6}$$

where R_y is the ***remaining*** nodal reaction. When $t=t_{end}$, (6) shows that the remaining nodal force is reduced to zero since $\Delta R_y=-R_y$.

2.2 Implementation

Constant crack growth rates were enforced under plane strain conditions for a compact specimen subjected to elastic and power-law secondary creep deformation according to $\dot{\epsilon}=\dot{\sigma}/E+A\sigma^n$ where E=207 GPa, $A=4.12(10)^{-25}$ MPa^{-10} hr^{-1} and n=10. Poisson's ratio was taken as 0.3. A constant external load of 4.45 kN was applied to the specimen whose width and thickness were both 2.54 cm. The initial and final crack lengths were 1.28 cm and 1.60 cm, respectively. The mesh consisted of 1354 - 4 noded isoparametric elements with a dense region of rectangular elements along the crack growth path where 50 crack growth increments were modeled. Relatively slow (0.000323 mm/hr) and fast (0.645 mm/hr) crack growth rates were enforced to simulate creep-ductile and creep-brittle crack extension, respectively. The total time of crack growth was 10,000 hours for the creep-ductile case and 5 hours for the creep-brittle case. An indication that creep-ductile and creep-brittle conditions were actually achieved is provided by the plot of $\dot{V}_c/\dot{V}$ in Figure 1. Most $\dot{V}_c/\dot{V}$ values were greater than 0.8 for the creep-ductile material and less than 0.4 for the creep-brittle material.

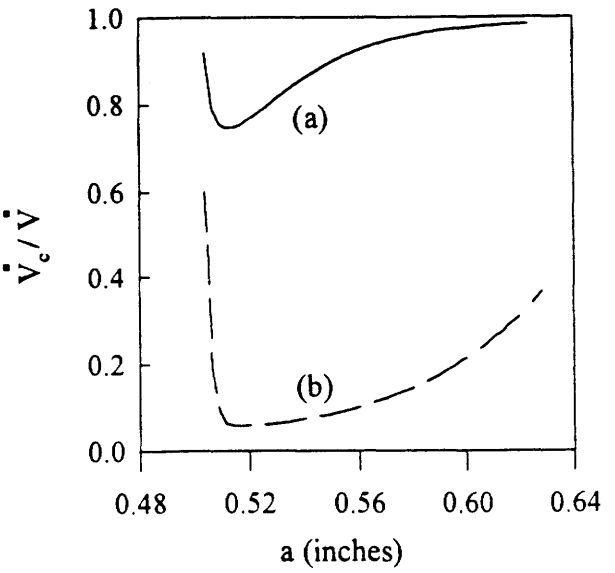

Figure 1 - $\dot{V}_c/\dot{V}$ ratios for (a) creep-ductile response and (b) creep-brittle response.

2.3 Visualization of Creep Zone Evolution

Understanding of the finite element results is enhanced using a visualization program, developed as part of this work, to simulate the evolution of various crack tip field parameters at different stages of crack growth. Figure 2 shows contour plots of the effective creep strain at three stages of crack growth for the creep-ductile and creep-brittle materials. The white areas of the filled contour plots denote regions where creep strains are greater than 0.002 while the black areas denote near zero creep strains.

(a) Creep-ductile results. The initial shape of the creep zone is more or less what would be predicted by stationary crack mechanics. However, as the crack tip stress field relaxes in the presence of crack growth, the near tip creep zone actually shrinks (this occurs between the first and second photo). Continued crack growth results in rapid accumulation of creep strain and the onset of extensive creep conditions.

(b) Creep-brittle results. Significant levels of creep deformation are limited to a thin region adjacent to the crack growth path. The characteristic "knob" observed near the initial crack tip is an artifact of the initially elastic crack tip fields which produce high creep strain rates. As the stresses near the crack tip relax, the driving force for creep

deformation decreases resulting in a corresponding decrease in the creep zone size. Both residual stress and residual creep strain are left in the wake of the crack. As the crack grows, the crack tip fields become more intense resulting in a growing creep zone in the vicinity of the crack tip and $\dot{V}_c$ values significantly larger than zero.

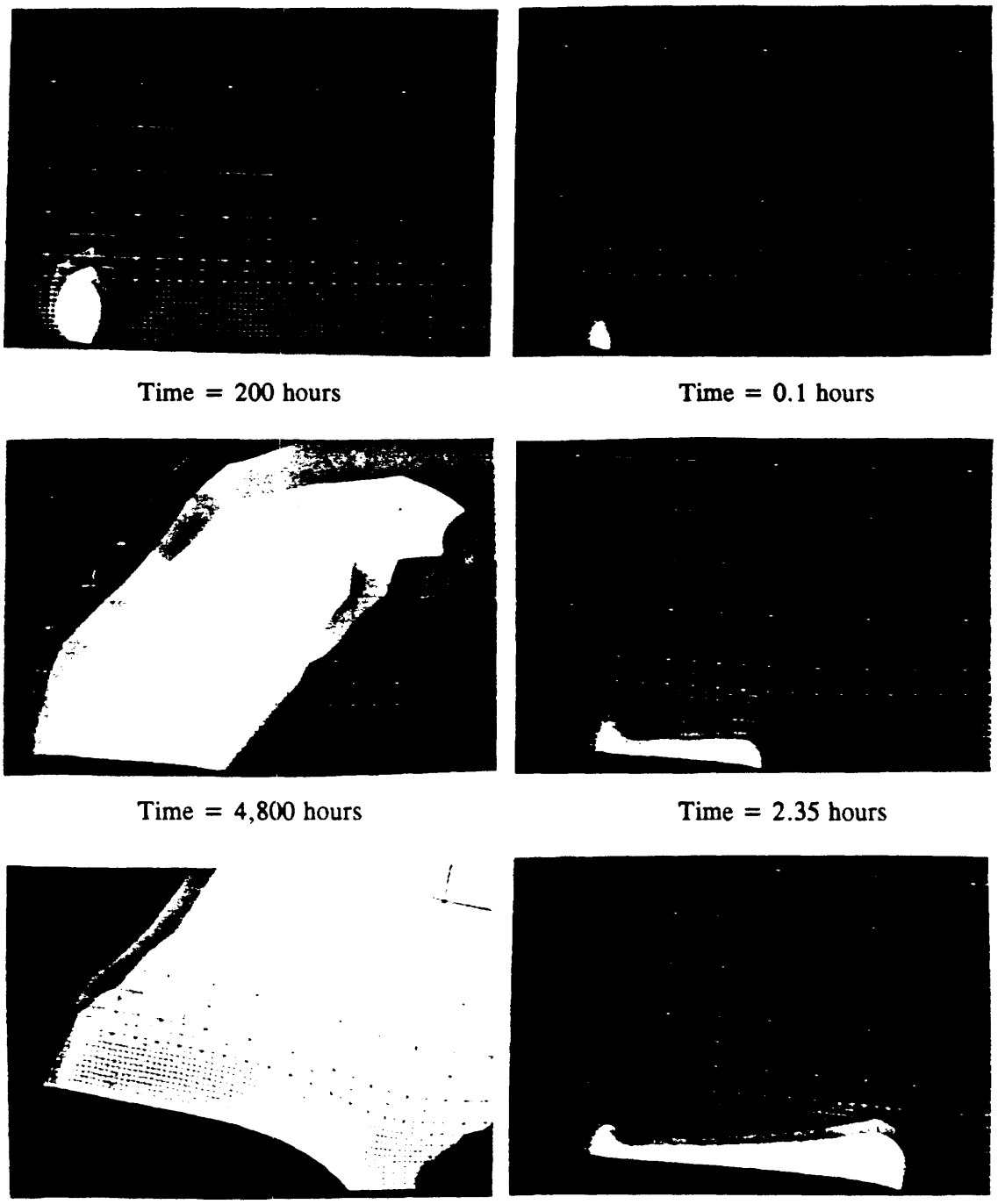

Time = 200 hours | Time = 0.1 hours

Time = 4,800 hours | Time = 2.35 hours

Time = 9,600 hours | Time = 4.7 hours

Creep-Ductile Response | **Creep-Brittle Response**

Figure 2 - Contour plots of effective creep strain at various stages of growth.

3. EFFECTS OF CRACK GROWTH ON THE LOAD-LINE DEFLECTION RATE

3.1 Numerical analysis and results

To determine the effect of residual creep deformation or "history" on the load-line deflection due to creep (V_c), the elastic/secondary creep finite element analyses above were interrupted after various amounts of crack growth and then allowed to proceed under purely elastic conditions. For example, one analysis allowed 10 elastic/secondary creep crack growth increments followed by 40 elastic crack growth increments. In all cases, V_c was computed as $V_c = V - V_e$ where V_e is computed analytically based on specimen compliance (given the initial load-line displacement).

History effects for creep-ductile crack growth are shown in Figure 3. This plot indicates that the effect of previously accumulated creep deformation on V_c remains intact as subsequent crack growth occurs. Consequently, the load-line deflection rate due to creep ($\dot{V}_c$) is related to the current rate of accumulation of creep deformation and not to history effects since $\dot{V}_c \approx 0$ for the elastic growth portions of the plot (the elastic growth lines are relatively horizontal).

History effects for creep-brittle crack growth are also shown in Figure 3. This plot indicates that the effect of previously accumulated creep deformation on V_c diminishes as residual creep deformation is left in the wake of the growing crack. Consequently, the load-line deflection rate due to creep ($\dot{V}_c$) is related to both the current rate of expansion of the creep zone and to the residual creep deformation left in the wake of the growing crack (values of V_c gradually approach zero as the residual deformation is left further and further behind the crack tip).

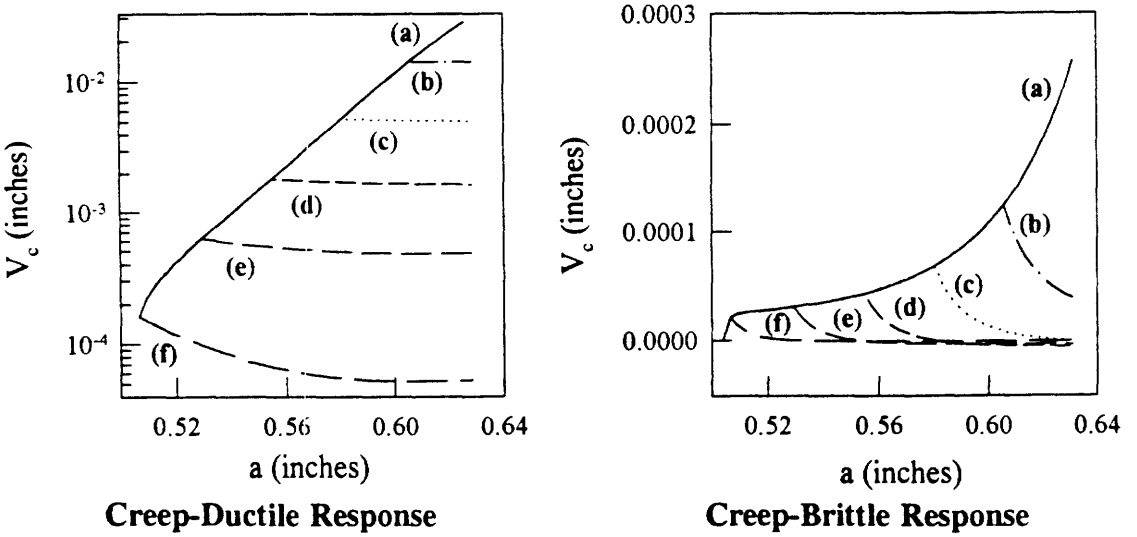

Figure 3 - Plots of V_c for various amounts of creep crack growth followed by elastic crack growth. The number of creep crack growth increments and elastic crack growth increments (creep/elastic) for each curve is (a) 50/0, (b) 40/10, (c) 30/20, (d) 20/30, and (e) 10/40, (f) 1/49.

These findings have important consequences for the analysis of creep-brittle crack growth. Experimental observation of negative values of $\dot{V}_c$ have been attributed to

experimental error or to a breakdown of deflection rate partitioning. While history effects provide a negative contribution to $\dot{V}_c$ (Figure 3), the expanding creep zone near the tip provides a positive contribution to $\dot{V}_c$. This suggests that negative values of $\dot{V}_c/\dot{V}$ are possible, depending on competing effects of history and the instantaneous rate of accumulation of creep deformation near the tip. These results demonstrate that the physical interpretation of fracture parameters based on $\dot{V}_c$, such as the C_t parameter [2], is somewhat different for creep-ductile and creep-brittle materials.

4. IMPLICATIONS OF DEFLECTION RATE PARTITIONING FOR $\dot{V}_c/\dot{V} \geq 0.8$

Although deflection rate partitioning may be used to quantitatively characterize material response as creep-ductile or creep-brittle, a comparison of the crack growth rate ($\dot{a}$) and creep zone expansion rate ($\dot{r}_c$) is often used to qualitatively define creep-ductile and creep-brittle response in the small-scale creep regime. Creep-ductile and creep-brittle crack growth are often defined as $\dot{r}_c >> \dot{a}$ and $\dot{r}_c \approx \dot{a}$, respectively.

When the crack tip fields evolve in a self-similar fashion, small-scale creep conditions apply, and history effects are negligible, limits can be placed on the minimum rate of expansion of the creep zone for validity of creep-ductile crack growth:

$$\frac{\dot{V}_c}{\dot{V}} = \frac{\dot{V}_c}{\dot{V}_e + \dot{V}_c} \geq 0.8 \qquad or \qquad \dot{V}_c \geq 4\dot{V}_e . \tag{7}$$

Using expressions for $\dot{V}_e$ and $\dot{V}_c$ in [2] results in $\dot{r}_c \geq 4\dot{a}/\beta$ where β is a numerically determined scaling factor. If β is taken as 1/3, as in earlier studies of creep-ductile materials [4], then $\dot{r}_c \geq 12\dot{a}$. This factor of 12 is in contrast to the conditions which exist for steady state creep-brittle crack growth where $\dot{r}_c \cong \dot{a}$.

Acknowledgements -- The support of this work by the NSF and NASA is gratefully acknowledged.

REFERENCES

[1] A. Saxena and J.D. Landes, Characterization of Creep Crack Growth in Metals, Advances in Fracture Research, Sixth International Conference on Fracture, Pergamon Press (1984), pp.3977-3988.

[2] A. Saxena, Creep Crack Growth Under Non Steady-State Conditions, Fracture Mechanics: Seventeenth Volume, ASTM STP 905 (1986), pp.185-201.

[3] K. Jones, The Creep Behavior of Aluminum Alloy 8009, Master's Thesis, Materials Engineering, Georgia Institute of Technology (1993).

[4] C.P. Leung and D.L. McDowell, Inclusion of Primary Creep in the Estimation of the C_t Parameter, International Journal of Fracture, Vol.46 (1990), pp.81-104.

[5] D.E. Hawk and J.L. Bassani, Transient Crack Growth Under Creep Conditions, Journal of the Mechanics and Physics of Solids, Vol. 34, No. 3 (1986), pp.191-212.

[6] E.T. Moyer, Jr. and H. Liebowitz, Creep Crack Growth Modeling and Near Tip Stress Fields, *Engineering Fracture Mechanics*, Vol. 28, No. 5/6 (1987), pp.601-621.